Università degli Studi di Ferrara

DOTTORATO DI RICERCA IN
FARMACOLOGIA E ONCOLOGIA MOLECOLARE

CICLO XXIII

COORDINATORE Prof. Antonio Cuneo

Transcription-independent effects of TGF-B on mitochondrial Ca^{2+} homeostasis

Settore Scientifico Disciplinare MED/04

Dottoranda
Dott.ssa Siviero Roberta

Tutore
Dott. Alessandro Rimessi

Anni 2008/2010

CONTENTS

ABSTRACT

The rapid response of mitochondria to cellular Ca^{2+} signals depends on their close proximity to the ER, allowing them to sense microdomains of high [Ca^{2+}] meeting the low affinity of the mitochondrial Ca^{2+} uniporter (MCU) of the inner membrane. Recent work has demonstrated that the subcellular fraction denominated Mitochondria-Associated Membranes (MAMs) may correspond to this signaling domain, as in electron micrographs it shows the apposition of the two organelles and it is enriched in Ca^{2+} channels and regulatory proteins. The Transforming Growth Factor-β (TGF-β) family consists of more than 30 different but structurally related polypeptides, which are known to have crucial roles in the regulation of cell proliferation, differentiation and apoptosis. The downstream effectors of TGF-β signaling are intracellular proteins called Smads that hetero-oligomerize after phosphorylation and subsequently migrate into the nucleus to influence gene expression. While much progress has been made in understanding TGF-β regulation of gene expression, the subcellular distribution of Smad proteins and their nuclear-independent activity are still incompletely understood.

We have investigated the effect of the TGF-β signaling on intracellular Ca^{2+} homeostasis. The results showed that Smad2/3, both in HeLa cells and in liver preparations, are present in mitochondria, with a specific enrichment in the MAM fraction. Such a distribution may underlie a direct, transcription-independent role in the modulation of the ER/mitochondria Ca^{2+} cross-talk. This possibility has been directly investigated using aequorin-based recombinant probes targeted to the mitochondria, the ER and the cytosol. Specifically, we observed that treatment with inhibitors of the TGF-β receptor family, such as SB431542 and Dorsomorphin (Compound C) reduces agonist-dependent increases of mitochondrial Ca^{2+} concentration $[Ca^{2+}]_m$, while leaving the cytosolic responses unaffected. The effects were observed also upon inhibition of protein

synthesis, thus ruling out the possibility that they are due to alterations of the expression levels of Ca^{2+} transporters. The same effects were observed by shRNA silencing of Smads, thus involving these TGF-β transducers in the mitochondrial effects. Work is currently under way to identify the mechanism of the Ca^{2+} signalling alterations (intrinsic desensitization of the MCU, reduction of the electrochemical driving force, etc.).

Altogether, these data demonstrate that also the TGF-β signaling pathway converges on mitochondrial checkpoint, clustering intracellular transducers in critical signaling domains and modulating Ca^{2+} loading and the sensitivity to growth-promoting and apoptotic challenges.

ABSTRACT (italiano)

La rapida risposta dei mitocondri ai segnali Ca^{2+} intracellulari dipende dalla loro prossimità al Reticolo Endoplasmatica che permette loro di sentire microdomini caratterizzati da elevate concentrazioni di Ca^{2+} che spiegano come questi organelli possano accumulare transitoriamente grandi quantità di calcio nonostante sia nota la bassa affinità con cui il trasportatore mitocondriale (MCU) sia in grado di muovere lo ione attraverso il doppio strato della membrana. Recentemente è stato dimostrato che la frazione subcellulare denominata MAM (Mitochondrial Associated Membrane) può corrispondere al dominio funzionale poiché in studi morfologici precedenti è stata osservata la giustapposizione dei mitocondri al Reticolo Endoplasmatico e inoltre tali regioni risultano arricchite di canali Ca^{2+} e proteine regolatrici. La famiglia del Transforming Growth Factor-β (TGF-β) consiste in più di 30 membri diversi, polipeptidi strutturalmente correlati con note proprietà regolatorie in processi cellulari come la proliferazione, il differenziamento e l'apoptosi. Gli effettori a valle del TGF-β sono proteine chiamate Smads che etero-oligomerizzano in seguito a fosforilazione e migrano nel nucleo dove regolano l'espressione genica. Mentre sono stati fatti molti progressi verso la comprensione dell'attività nucleare del TGF-β, la distribuzione subcellulare e l'attività nucleo-indipendente delle Smads risulta ancora piuttosto sconosciuta. In questo lavoro è stato investigato il ruolo di TGF-β nell'omeostasi intracellulare del Ca^{2+} .

I risultati dimostrano una localizzazione subcellulare delle Smads nei mitocondri sia in HeLa che in preparazioni da fegato di topo, mostrando un particolare arricchimento a livello delle MAMs. Questa distribuzione può suggerire un ruolo trascrizione-indipendente di queste proteine nella regolazione del cross-talk tra Reticolo Endoplasmatico e mitocondri. Tale ipotesi è stata testata direttamente grazie all'utilizzo di sonde per il Ca^{2+} che sfruttano la tecnologia dell'aequorina,

targhettate in modo specifico ai mitocondri, al Reticolo Endoplasmatico e al cytosol. Precisamente è stato osservato che l'utilizzo di inibitori di isoforme diverse del recettore per il TGF-β, come la molecola SB431542 e Dorsomorphin (Compound C) riduce l'ingresso di calcio nei mitocondri, lasciando inalterata la risposta nel cytosol. La stessa osservazione è stata fatta in presenza di un inibitore della sintesi proteica, eliminando così la possibilità che tale effetto fosse il risultato di un'alterazione nei livelli di espressione dei trasportatori mitocondriali del Ca^{2+}. Lo stesso effetto è stato osservato mediante l'uso di ShRNA capaci di silenziare diverse isoforme di Smads.

La comprensione del meccanismo alla base dell'alterazione mitocondriale osservata è ancora in fase di studio. I risultati di questo lavoro mostrano comunque che anche la cascata del segnale di TGF-β converge al checkpoint mitocondriale regolando la distribuzione di trasduttori intracellulari a livello di domini funzionali critici e modulando l'uptake di Ca^{2+} nella matrice mitocondriale e la sensibilità degli organelli a segnali di tipo proliferativo o apoptotico

INTRODUCTION

Mitochondria: key regulators of intracellular calcium homeostasis

Mitochondria are intracellular organelles characterized by a double membrane and a circular double-stranded DNA molecules. The double membrane is composed by a plain outer layer, which allows the passage of ions and metabolites up to 5000 Da and the more selective inner membrane, characterized by invaginations, the so called *cristae.* Between these two very different layers the mitochondrial matrix is enclosed. The mitochondrial DNA is a 16.6 Kb molecule and it encodes 13 proteins all of which are known to be part of the mitochondrial Electron Transport Chain (mETC). Thanks to their biosynthetic capacities mitochondria have central role in the supply of the high amount of energy required for many different cellular functions such as hormones synthesis and secretion, muscle contraction, proliferation, biomolecules synthesis and maintenance of ionic gradient across the membrane. Substrates derived from other intracellular processes such as glycolysis or the fatty acid metabolism, are converted to Acetyl-CoA which enters the Tricarboxilic Acid Cycle TCA and its complete degradation is coupled with the production of NADH and $FADH_2$. These new molecules are the effective electron donors for the mETC which is composed of five different complexes: complex I (NADH dehydrogenase), complex II (succinate dehydrogenase), complex III (ubiquinol cytochrome c reductase), complex IV (cytochrome c oxidase) and complex V that constitutes the F1F0-ATP synthase. While electrons are transferred from NADH and $FADH_2$ to these complexes, energy is stored as an electrochemical gradient across the inner membrane which explains the existence of a negative mitochondrial membrane potential (-180mV against the cytosol). The F1F0-ATP synthase can make the H^+ cross the inner membrane to reenter the matrix coupling the energy derived from the proton gradient with the phosphorylation of ADP into ATP

(according to the so called chemiosmotic principle). The new ATP molecules are now ready to leave the mitochondria first from the inner membrane through the Adenine Nucleotide Transferase (ANT) which exchanges it with ADP (to provide new substrate for the F1F0-ATP synthase) and then through a mitochondrial channel of the outer membrane called VDAC.

In the last few decades many different groups are engaged in the comprehension of new roles for mitochondria which have shown to be involved in other cellular mechanisms such as amino-acid synthesis, lipid metabolism, reactive oxygen species production (ROS), cell death and, most importantly for the present work, Ca^{2+} signaling. Therefore any mitochondrial dysfunction is at the basis of pathological conditions like neurodegenerative diseases such as Alzheimer's and Parkinson's, motoneuron disorders such as amyotrophic lateral sclerosis, autosomal dominant optic atrophy, diabetes, ageing and cancer. Thus it is evident how much importance has the understanding of the role of mitochondria in the cohordination of cytosolic and other subcellular organelles signals.

Calcium signaling: a general overview

Ca^{2+} is one of the most described intracellular second messenger (Hajnoczky G., 2000) and this is the reason why its cytosolic concentration $[Ca^{2+}]_c$ is taken under strict control by many different pumps, channels, exchangers and binding proteins. Actually $[Ca^{2+}]_c$ is maintained around value of 100nM (while the extracellular $[Ca^{2+}]$ is 1mM) by the activity of the Plasma membrane Ca^{2+}-ATPase (PMCA) which pump Ca^{2+} outside the cells and of the Na^+/Ca^{2+} exchanger (NCX). The increased of the intracellular $[Ca^{2+}]$ is mainly due to its liberation from intracellular stores (Endoplasmic Reticulum and Golgi apparatus) or the entry from the extracellular medium.

The most important intracellular Ca^{2+} store is the ER which is characterized by the presence on his membrane of the IP_3 Receptor (IP_3R) a channel which exposes the binding site for IP_3 on the

cytosol and forms a transmembrane channel across the ER membrane. Ca^{2+} is released from the ER upon IP_3R stimulation by IP_3 that derives from the hydrolysis of phosphatidylinositol 4,5 bisphosphate (PIP2) carried out by Phospholipase C (PLC) which, in its turn, is activated by ligand binding to G-coupled receptors on the plasma membrane. Intracellular store depletion activates an inward current from the extracellular space, the so called capacitative Ca^{2+} entry (CCE) which molecular mechanism has been recently explained, with the involvment of an ER Ca^{2+} sensing protein (STIM) and a Ca^{2+} channel on the plasma membrane ORA1 (Oh-hora M. and Rao A., 2008).

Three classes of Ca^{2+} channel on the plasma membrane are also responsible of intracellular Ca^{2+} increased: the Voltage Operated Ca^{2+} channels (VOCs) which open following a decrease of membrane potential (Bertolino M. and Llinas R.R., 1992), the Receptor Operated Ca^{2+} channels (ROCs), also called ligand gated channels, which open following the binding of an external ligand (McFadzean I. and Gibson A., 2002) and the Second Messenger Operated Channels (SMOCs) which open following the binding of a second messenger on the inner surface of the membrane (Meldolesi J. and Pozzan T., 1987). Ca^{2+} has to be rapidly removed once it has exerted its second messenger function and mechanisms for its extrusion are PMCA and NCX but also pumps capable to refill the intracellular stores such as Sarco-Endoplasmic Reticlum Ca^{2+} ATPases (SERCAs).

Mitochondria can rapidly accumulate Ca^{2+} thanks to the electrochemical gradient established by the movement of protons across the inner mitochondrial membrane (IMM), however the development of specific probes for the measurement of $[Ca^{2+}]$ in the mitochondria revealed a capacity of uptaking the ion much higher if compared with the affinity of $[Ca^{2+}]$ transporter, this is the reason why today it is generally accepted the idea of a strategic close proximity of a mitochondrial fraction able to sense short but large $[Ca^{2+}]$.

Mitochondria cohordinate Ca^{2+} signaling

By the end of 70's mitochondria were thought to be intracellular Ca^{2+} stores, indeed according to the chemosmotic theory these organelles could exploit the H^+ electrochemical gradient to produce ATP but also to accumulate cations into the matrix. Ca^{2+} transfer across the ion-impermeable membrane is in fact not due to the activity of pumps or exchangers but it is mediated by a "uniporter" which molecular identity has not been completely described yet and the electrochemical potential gradient across the mitochondrial membrane (-180mV negative to the cytosol) drives it (Gunter T.E., 1998). Moreover if Ca^{2+} accumulation into the matrix was due to thermodynamic parameters, according to the Nerst equation, equilibrium would be reached only when $[Ca^{2+}]$ in the matrix reaches value 10^6 higher than in the cytosol.

Only a decade later, researchers discovered that the $[Ca^{2+}]_m$ was lower than expected, this notion and the discovery of a new intracellular organelle the Endoplamic Reticulum (Streb H., 1983) made evident that mitochondria were not a Ca^{2+} store.

At the end of the 80s the general idea was that mitochondria could not accumulate significant amount of the cations considering the low affinity of their uniporter and the low values of the $[Ca^{2+}]_c$, around 0.1 µM in normal conditions and 1-3 µM under stimulation.

Nevertheless three mitochondrial enzymes (pyruvate-, α-ketoglutarate and isocitrate dehydrogenase) were regulated by Ca^{2+} oscillations but the demonstration of this idea had to wait until the early 90s. Indeed the direct measurement of Ca^{2+} transients within the mitochondrial compartment was possible only in 1990s, when Rizzuto and coworkers introduced the Ca^{2+}-sensitive probe aequorin, which could be targeted to mitochondria and other intracellular organelles. These studies demonstrates in many different cellular type that the mitochondrial ability of uptaking Ca^{2+} was much more higher than expected (ranging from 10µM to 500µM).

Taking into consideration the low affinity of mitochondrial uniporter and the low concentration of Ca^{2+} in the cytosol. This discrepancy lead the researchers to the formulation of the "hotspot hypothesis" according to which mitochondria could sense microdomains of high [Ca^{2+}] achieved through close proximity between a fraction of mitochondria and the ER.

The release of Ca^{2+} from the latter happens through the IP_3 channels on its surface and this creates a microenviroments where [Ca^{2+}] is much higher than that measured in the bulk cytosol (Rizzuto R., 1993). Few years later a strong evidence in support of the "hotspot hypothesis" was that collected by Griffiths and coworkers, who observed that in cardiac cells concentrations of Ca^{2+} chelator EGTA that could abolish Ca^{2+} cytosolic transient, could not inhibit Ca^{2+} transient into the mitochondria, this experiment suggested that the distance was so small that the cations could diffuse from ER to mitochondria more rapidly than it can be buffered by EGTA.

The idea of a cross-talk between the two organelles was recently demonstrated by fast single-cell imaging with targeted Ca^{2+} sensitive GFPs (pericams and cameleons) and supported by the observation that $[Ca^{2+}]_m$ spikes originates from a discrete number of sites and rapidly diffuse through the mitochondrial network (Szabadkai G., 2004).

Endoplasmic Reticulum/mitochondria physical contacts: the MAMs microdomains

The existence of a subdomain of the ER (Endoplasmic Reticulum) that comes into transient contact with mitochondrial outer membranes, has been deeply demonstrated in mammalian cells and described as a functional site of the import of PS (Phosphatidylserine) into mitochondria (Vance JE., 2008).

Close appositions between ER and mitochondria have been observed thanks to the analysis of electron micrographs (EM) in fixed samples of many different cell types while experiments performed in living cells by Rizzuto and coworkers had eventually confirmed the physical and

functional coupling of these two organelles, by labelling the two organelles with targeted spectral variants of GFP (mtBFP and erGFP) (Rizzuto R., 1998). These experiments revealed the presence of overlapping regions of the two organelles (thus establishing an upper limit of 100 nm for their distance) and allowed to estimate the area of the contact sites as 5-20% of total mitochondrial surface. More recently, electron tomography studies allowed to estimate an even smaller distance (10-25 nm) and revealed the presence of trypsin-sensitive (hence proteinaceous) tethers between the two membrane (Csordas A., 2006).

The specific mitochondrial regions showing close proximity to the ER cisternae are referred to as MAMs (Mitochondrial Associated Membranes) (Vance JE., 1990) and being the headquarters of lipid transfer contain several phospholipids and glycosphingolipid-synthesizing enzymes such as Fatty Acid CoA ligase 4 (FACL) as well as those enzymes involved in PS synthesis pathway.

MAMs are also involved in rapid movement of Ca^{2+} ions between the two organelles, playing a fundamental role in the coordination of ATP production through the activation of the mitochondrial dehydrogenases as well as the activation of the cell death program (Berridge M. J., 2002) .

The shaping of the ER-mitochondrial network can be affected by bounding proteins and physiological ligands; recently Hajnoczky and coworkers demonstrated that exposure to TGFβ affects Ca^{2+} transfer to the mitochondria.(Hajnoczky G., 2008).

Unfortunately, very few of the relevant scaffolding or signaling proteins of the ER/mitochondria contacts have been identified, despite the growing interest on the topic. Nevertheless, novel candidates have being rapidly isolated, and are under scrutiny. Thus it can be envisaged that the molecular characterization will rapidly proceed thanks to the validation of biochemical approaches for the isolation of ER/mitochondria contacts.

Indeed a known technical pitfall of subcellular fractionation, i.e. the “contamination” of the mitochondrial fraction with ER vesicles, has been demonstrated to be due to the actual co-segregation of stably associated mitochondrial and ER membranes. This has led to a more accurate separation, by gradient centrifugations, of pure mitochondria from a “mitochondria-associated membrane” (MAM). This is the fraction enriched in enzymes involved in lipid and glucose metabolism and in signalling proteins (such as the IP_3Rs), and thus representing the biochemical counterpart of the ER/mitochondria units revealed in the signaling studies (Vance J.E., 1990). More recently, the same subcellular fraction has been shown to contain as well Ca^{2+} signaling elements of both organelles (Szabadkai G., 2007), thus supporting its central role in ER (or SR)/mitochondria crosstalk .

The molecular scenario is gradually adding new information, and we will here cite a couple of interesting examples, involving chaperones. The role of glucose-regulated protein 75 (grp75) within the mitochondrial matrix as a molecular chaperone assisting the refolding of newly imported proteins, was well established. It was then reported that a pool of grp75 is not imported into the matrix, but has a cytosolic distribution. Previous works carried out in our lab identified, in two hybrid screenings, grp75 as a VDAC interactor, and demonstrated that it can mediate the molecular interaction of VDAC with the IP_3R, allowing a positive regulation of mitochondrial Ca^{2+} uptake. This implies a sort of conformational coupling between the Ca^{2+} channels of the two organelles, and highlights the importance of macromolecular complexes located in the MAM for this functional interaction (Colombini M., 2004). The second interesting example is that of sigma-1, a novel ER chaperone serendipitously identified in cellular distribution studies which shown to be involved in the Ca^{2+}-mediated stabilization of IP_3Rs. Sigma-1 receptor is normally localized in MAM, bound to another ER chaperone (BiP). When the luminal Ca^{2+} concentration of the ER drops, following the opening of IP_3Rs, sigma-1 dissociates from BiP and binds to type 3 IP_3R, thus

preventing its degradation by the proteasome. Thus, sigma-1 appears to be involved in maintaining, from the ER luminal side, the integrity of the ER/mitochondrial Ca^{2+} cross-talk in conditions (e.g. ER stress) that could impair signal transmission, and hence control of cellular bioenergetics. In 2005, Simmen et al. reported the identification of a multifunctional sorting protein PACS-2, that integrates ER-mitochondria and apoptosis signaling, depletion of this protein causes mitochondrial fragmentation and uncoupling from ER, influencing Ca^{2+} homeostasis. Moreover in response of apoptotic stimuli, PACS-2 has been demonstrated capable of inducing Bid recruitment to mitochondria, event that leads to cytochrome c release and caspase 3 activation.

The dynamical interconnection between the two organelles involves a family of "mitochondria-shaping proteins" such as the dynamin-related GTPase DRP1, required for the mitocondria-ER fission, or the GTPase called Optic Atrophy 1 (OPA 1) crucial for the so called mitofusion. Along this line, Scorrano and coworkers have recently pointed out the crucial role of the mitofusin (MFN 1 and 2), in particular the isophorm 2 is thought to be important for ER-mitochondrial interactions engaging them both in homo and etero-complexes. (Scorrano L., 2008). They showed how the distance of two organelles is increased where MFN 2 lacks and how it impairs mitochondrial Ca^{2+} uptake, giving solid evidence in support to the microdomains theory. Moreover the ER-mitochondrial apposition performed by MFN 2 predispose mitochondria to high Ca^{2+} microdomains and the consequent overloading, leading eventually to apoptosis by excessive Ca^{2+} transfer.

Integration of the TGF-B pathway into the cellular signaling network

Transforming growth factor–β (TGF-β) is a secreted cytochine that exerts an amazing diversity of biological effects including proliferation, differentiation, migration and apoptosis. The superfamily of TGF-β proteins comprises more than thirty members, the most important being TGF-β itself,

bone morphogenetic proteins (BMPs), activins and differentiation growth factors (GDFs). (Massaguè J. 1998).

Considering the limited assortment of transmembrane receptors and downstream signaling molecules, the pivotal nature of TGF-β asks for a great flexibility of the signaling cascade, this is achieved thanks to a complex network of mechanisms that control the activation of TGF-β in the extracellular space to modulate transcriptional activation in the nucleus.

The variability of this pathway is generated by cell and tissue-specific composition, interaction of receptors, signal transducers, DNA-binding partners and finally the cross-talk with regulators from other pathways.

TGF-β signal transduction: the basics

Three human isoforms of TGF-β (TGF-β1, TGF-β2, TGF-β3) are synthesized as large precursor which is processed to obtain the mature protein. Bioactive TGF-β homodimers signal through transmembrane serine/threonine kinase receptors designated as TGF-β Receptor type I (TBRI) and type II (TβRII) (Frazen P. 1993). Initial binding to the constitutively active TβRII is followed by recruitment of TβRI into a heteromeric complex. Subsequent transphosphorylation of TβRI at the serine rich region, the so called GS-box, is mediated by TβRII and leads to activaton of TβRI. Interestingly TβRI activation is not due to an increase of actual kinase activity but is rather based on the creation of a binding site for Smad proteins which represent the substrates for TβRI (Huse M. 2001). A key determinant of TβRI-Smad interaction is represented by a region located in the kinase domain of TβRI called L45-loop. Within the L45-loop four amino acids that differ in TGF-β and BMP type I receptors, confer specificity for distinct Smad isoform and thus separate TGF-β and BMP pathways (Persson U. 1998).

Smad proteins can be divided into three subfamilies: receptor-activated Smads (R-Smads) including BMP-activated Smads (smad1, Smad5 and Smad8) and TGF-β activated Smads (Smad2 and Smad3), the common mediator Smad4 (Co-Smad) and finally the inhibitory Smad6 and Smad7 (I-Smads) (Heldin C.-H. 1997). TβRI causes R-Smad phosphorylation at the C-terminal SSXS-motif which is conserved among all R-Smads thereby causing dissociation from the receptor and heteromeric complex formation with Smad4 (Massaguè J. 2000). Smad complexes translocate to the nucleus, assemble with specific DNA-binding co-factors and co-modulators to finally activate transcription. The choice of target genes is thereby determined by the composition of the transcriptional complex.

The Transforming growth factor-β signaling receptors

In mammals only five type II receptors and seven type I receptors have been identified for ligand belonging to the large TGF-β superfamily. They all are transmembrane receptors that contain an intracellular serine/threonine kinase domain.

The most described signaling receptors for TGF-β are TGF-β type II receptors (TGF-βRII) and the TGF-β type I receptor (TGF-βRI). In addition, two other TGF-β binding proteins called betaglycan (or TGF-βRIII) and endoglin are frequenty involved in formation of receptor complexes and function predominantly in ligand presentation. However as shown in table 1, the repertoire of TGF-β receptors is supplemented by other receptors or splice variants of the receptors that are also capable of transducing signals in response to TGF-β. Thus, signal diversity may be generated by different receptor combinations.

In addition to TGF-β RI , there are other type I receptors such as ALK1 and ALK2 that transmit signals evoked by TGF-β. Pathological relevance is reflected by the linkage of mutations in both the endoglin and the ALK1 gene to an autosomal dominant disorder named hereditary hemorrhagic

teleangiectasia (HHT). Moreover ALK1 plays an important role during vascular development. ALK2 is similar to ALK1 because it binds TGF-β following interaction with TGF-β receptor II and an accessory receptor and conveys the signal via the BMP-Smads, Smad1 and Smad5 respectively (Lai Y.T., 2000).

Referring to type II receptors, it has a splice variant, TβRII-B which contains an insertion of 25 aminoacids in the extracellular part of the receptor and shows functional differences. An outstanding physiological relevance for TβRII-B expression is therefore predicted for tissue such as bone, in which TGF-β2 represents the major TGF-β isoform.

The major TGF-β-binding molecule on most cell type is TβRIII also called betaglycan, it is a transmembrane proteoglycan that is able to bind all three TGF-β isoforms via two independent binding sites in the core protein. TβRIII exerts its function in presenting TGF-β2 to TGF-βRII which shows only low intrinsic affinity for TGF-β2. In contrast to the facilitation of ligand access to the receptors, the soluble secreted domain of TGF-βRIII has antagonistic effects through binding and sequestering the ligand. The short cytoplasmic domain is rich in serines and threonines which represents suitable sites for phosphorylation. Indeed a previous report describes that phosphorylation of the cytoplasmic domain by autophosphorylated TGF-βRII initiates the release of TGF-βRIII from the active signaling complex, consisting in TGF-βRI and II and the bound ligand.

A receptor variant that cross-regulates pathways of different members of the TGF-β family is represented by BMP and activin membrane bound inhibitor, this inhibitor is a pseudoreceptor similar to type I receptor apart from the lacking cytoplasmic kinase domain. Its capacity to associate with various type I receptor prevents the formation of functional homodimeric type I receptor complexes and thus causes abrogation of BMP as well as TGF-β and activin–mediated signaling.

In conclusion the repertoire of signaling receptors gives rise to multiple hetero-oligomeric receptor complexes and each of the involved receptor variants depicts a distinct expression pattern, ligand isoform specificity and ligand affinity, thus expanding signal diversity.

Distribution of different receptors

The overall distribution of the TGF-β receptors is functional to the formation of different oligomeric units. TβRI, TβRII, TβRIII have all been found as homo-oligomers already in the absence of TGF-β (Henis Y.I., 1994), in addition heteromeric complexes consisting of TβRII, TβRIII could be detected in absence and in presence of TGF-β. Based on their affinity for each other, a small but detectable proportion of TβRI-TβRII heteromeric receptor complexes exists in unstimulated cells. The fraction of these heteromeric complexes is significantly increased by ligand binding to TβRII which causes subsequent recruitment of TβRI.

The resulting tetrameric complexes consist of two molecules each of TβRI and TβRII and represent the actual signaling entity (Luo K., 1997). Homomeric receptor complexes are not sufficient to propagate TGF-β responses but are considered to be functionally important for regulating receptor kinase activity, as reported in the case of intermolecular autophosphorylation at multiple serine residues of TβRII (Luo K., 1996).

The ligand binding to TGF-β receptor triggers not only signaling but also initiates internalization of both ligand and receptor, in fact in absence of TGF-β, receptors are constantly internalized and recycled back to the membrane. Various proteins have been identified as capable of regulating TGF-β signaling. The basal receptor activity is kept under tight control by immunophilin FKBP12 (Wang T.1994), by binding the unphosphorylated GS-box of TβRI, FKBP12 stabilizes a conformation of TGF-βRI that is incapable of getting transphosphorylation by TGF-BR II thus preventing ligand-independent signaling. Ligand binding to TGF-βRII however induces conformational changes that

lead to displacement of FKBP12 and subsequent TGF-βR I activation by TGF-βR II (Huse M., 2001). Smad Anchor for Receptor Activation SARA has a binding domain for R-Smads and the C-terminal part which directly interacts with the activated TGF-BR I. The cooperative binding of SARA proteins enables the Smads phosphorylation by TGF-βR I which is followed by the dissociation of them from SARA and formation of heteromeric complex with Smad4.

The Disabled-2 protein Dab2 (Hocevar B.A., 2001) facilitates TGF-β signaling by bridging the receptors complex to the Smad proteins thanks to its N-terminal phosphotyrosine binding site PTB that is likely to allow association to the MH2 domain of Smad2 and Smad3.

The TβRI-Associated Protein-1 TRAP-1 associates with Smad4 attracting the co-Smads to the vicinity of receptors thus facilitating heteromeric complex formation between activated R-Smads and Smad4.

Negative regulation of TGF-β signaling is achieved by the inhibitory Smad7 (Nakao A., 1997), serine/threonine kinase receptor-associated protein STRAP or the Smad ubiquitination regulatory factors Smurf1 and 2. Smad7 lacks the SSXS-motif and so it is not a substrate for TβRI but it stably interacts with the activated receptor thereby competing with other R-Smads. STRAP was described to interact with both TβRI and TβRII and stabilizes the binding between TβRI and Smad7. Smurf proteins are bridged to the receptor by Smad7 and the ubiquitination of Smad7 leads to subsequent proteasomal and lysosomal degradation of the complex containing Smad7 and the TβRs.

Downstream effectors of TGF-β pathway: the Smad proteins

Smad proteins are so far the only known substrate for TβRs capable of transmitting the signal directly from the receptors to the nuclear transcriptional machinery.

Members of Smad family can be subdivide on the basis of their structural and functional properties: i) *receptor activated Smads* (R-Smads: Smad1, Smad5 and Smad8 (BMP activated); Smad2 and Smad3 (TGF-β activated) that become phosphorylated by type I receptors, ii) *common mediator Smad* (Co-Smad: Smad4) which oligomerizes with R-Smads and iii) *the inhibitory Smads* (I-Smads: Smad6 and Smads7) which antagonize TGF-β or BMP signals by competing with R-Smads for type I receptor activation (Massaguè J., 1998).

The overall structure of R-Smads and Co-Smads comprises the highly conserved N-terminal Mad homology 1 domain, MH1, and the C-terminal Mad homology 2 domain, MH2, which form globular structures, I-Smads contain the conserved MH2 domain but show little similarity in the N-terminal (Itoh S., 2000). Smad proteins have no intrinsic enzymatic activity and exert their role exclusively by protein-protein or DNA-protein interactions. The MH1 domain mediates autoinhibition by physically interacting with the MH2 domain, impeding its function in the absence of ligand, moreover the MH1 domain is necessary also for the ability to bind directly to DNA. The crystal structure of Smad proteins reveal that MH1 domain contains the hairpin-loop which is responsible for binding the DNA helix (Shi Y., 1998). Protein-protein interactions with transcription factors such as ATF2, c-Jun, SP1 or TFE3 are also mediated by MH1. This is the domain containing the nuclear localization signal NLS, for instance phosphorylation of Smad3 causes conformational changes that exposes its NLS-like motif allowing interaction with importin-β and recognition by the nuclear import machinery. Ligand-induced release of SARA unmasks the NLS motif and leads to Smad nuclear translocation by a mechanism independent of importin-β but requiring the MH2 domain.

The cytoplasmic localization of Smad4 is based on active nuclear export signal NES, its nuclear entry presupposes inactivation of NES which is achieved by hetero-oligomerization with R-Smads (Pierreux C.E., 2000).

Recent publications suggest that Smad1 and Smad2 upon ligand induced phosphorylation assemble to form a homotrimer which is stabilized by the MH2 domain of the neighbouring monomer, however formation of heterotrimer is energetically favoured over the homotrimer formation.

TGF-β induced activation of TGF-βRI is followed by transient interaction between TGF-βRI and R-Smads which are phosphorylated in the last two serine residues within the C-terminal SSXS-motif, consequently Smad proteins are released from their retention such as SARA, as well as TGF-βRI and the affinity for Smad4 is increased. Several lines of evidence show that Smads are the substrates also for the ERK subfamily of MAP kinases which are activated by the hepatocyte growth factors or epidermal growth factors. Nuclear accumulation of Smad2 was demonstrated to be affected by Ca^{2+}-calmodulin-dependent protein kinase II which triggers phosphorylation of several serine residues of Smad proteins (Wicks S.J., 2000). Protein Kinase C activated by TGF-β, provides a negative feedback by phosphorylating specific serine residues in the MH1 domain of Smad3 thus precluding its ability to bind the DNA. Further cytoplasmic kinases mediating Smad phosphorylation is the c-Jun N-terminal kinase JNK. TGF-β stimulates JNK and it leads to the phosphorylation of Smad3 at sites other than the SSXS motif, facilitating the following phosphorylation by TGF-βR I.

Several proteins negatively regulate TGF-β signaling , first of all inhibitory Smads rapidly induced by TGF-β, block phosphorylation of Smads, second Smad binding proteins and transcriptional co-repressors, third the Smurf proteins that target Smads for degradation, however the most obvious mechanism is the dephosphorylation of R-Smads after prolonged TGF-β stimulation.

TGF-β and Mitochondrial function

A functional relationship between TGF-β signaling and mitochondria has already been established by many different groups, for instance in regulating the intrinsic pathway of apoptosis. Gottfried et al. demonstrated that ARTS, a proapoptotic protein localized in the mitochondria, is essential for TGF-β-induced programmed cell death (Gottfried Y., 2004). In epithelial cell it has been observed that TGF-β treatment causes generation of reactive oxygen species and the consequent loss of mitochondrial membrane potential ($\Delta\psi$) which leads to activate the programmed cell death (Wang F., 2008). Clybouw et al. in 2008 showed that in early stages of tumor progression, TGF-β mediates apoptosis of epithelial and hepatocyte cells by leading Bim (a proapoptotic member of the BH3-only proteins) at the mitochondrial surface where it associates with Bcl-2 or Bcl-xL. The sequestration of these prosurvival members of the Bcl-2 family by Bim allows the activation of the apoptotic regulators Bax and Bak (Clybouw C., 2008). Moreover mutations in specific TGF-β family members proved to be linked to altered mitochondrial energy metabolism and oxygen consumption rate. (Liunan L., 2009).

Recently a new potential role has been demonstrated for TGF-β in the impairment of normal mobilization of intracellular Ca^{2+} stores (McGowan T.A., 2000), prior studies showed the reduction in IP_3R1 Ca^{2+} release in diabetic aortic and proglomerular smooth muscle cells which is indeed mediated by TGF-β (Sharma K., 2003). Thus the impairment of vascular cell dysfunction has been directly linked to the IP_3 –cytoplasmic Ca^{2+} signaling.

A key aspect of endoplasmic reticulum (ER) Ca^{2+} release is its coupling with the mitochondria (Rizzuto R. and Pozzan T., 2006) and Ca^{2+} mobilized through the IP_3 receptors or ryanodine receptors is effectively transferred to the mitochondria and stimulates, in the mitochondrial matrix, the ATP production.

Mitochondrial Ca^{2+} uptake exerts positive and negative feedback effects on the IP_3 receptor-mediated ER Ca^{2+} mobilization and affects SERCA pump-mediated ER Ca^{2+} reuptake. Moreover mitochondrial Ca^{2+} uptake regulates the mitochondrial phase of cell death, thus a well described binding between Ca^{2+} overload in the mitochondrial matrix and the activation of the apoptotic process has been already understood. Since TGF-β has been implicated as a key factor in many cellular processes, many different groups have been doing great efforts to understand the mechanism by which TGF-β may affect ER-mitochondrial communication.

AIMS

In the present study we observed a close relationship between the presence of the downstream effectors of TGF-β cascade in specific mitochondrial functional sites and the shaping of mitochondrial calcium homeostasis. Mitochondria can sense microdomains of high [Ca^{2+}] thanks to their close proximity to the ER. Recent work has demonstrated that the subcellular fraction denominated Mitochondria-Associated Membranes (MAMs) may correspond to this signaling domain which happen to be enriched in Ca^{2+} channels and regulatory proteins. The Transforming growth factor-β is known to have crucial roles in the regulation of cell proliferation, differentiation and apoptosis. The downstream effectors of TGF-β signaling are intracellular proteins called Smads that hetero-oligomerize after phosphorylation and subsequently migrate into the nucleus to influence gene expression. While much progress has been made in understanding TGF-β regulation of gene expression, the subcellular distribution of Smad proteins and their nuclear-independent activity are still incompletely understood.

We have investigated the effect of the TGF-β signaling on intracellular Ca^{2+} homeostasis. The results showed that Smad2/3, both in HeLa cells and in liver preparations, are present in mitochondria, with a specific enrichment in the MAM fraction. Such a distribution may underlie a direct, transcription-independent role in the modulation of the ER/mitochondria Ca^{2+} cross-talk. This possibility has been directly investigated using aequorin-based recombinant probes targeted to the mitochondria, the ER and the cytosol. Specifically, we observed that treatment with inhibitors of the TGF-β receptor family, such as SB431542 and Dorsomorphin (Compound C) reduces agonist-dependent increases of mitochondrial Ca^{2+} concentration $[Ca^{2+}]_m$, while leaving

the cytosolic responses unaffected. The effects were observed also upon inhibition of protein synthesis, thus ruling out the possibility that they are due to alterations of the expression levels of Ca^{2+} transporters. The same effects were observed by shRNA silencing of Smads, thus involving these TGF-β transducers in the mitochondrial effects. Work is currently under way to identify the mechanism of the Ca^{2+} signalling alterations (intrinsic desensitization of the MCU, reduction of the electrochemical driving force, etc.).

Altogether, these data demonstrate that also the TGF-β signaling pathway converges on mitochondrial checkpoint, clustering intracellular transducers in critical signaling domains and modulating Ca^{2+} loading and the sensitivity to growth-promoting and apoptotic challenges.

MATERIALS AND METHODS

Aequorin: a Ca^{2+} sensitive probe

Aequorin is a 21 KDa protein isolated from jellyfish of the genus Aequorea which emits blue light in presence of calcium ions. The aequorin originally purified from jellyfish is a mixture of different isoforms called "heterogeneous aequorin" (Shimomura O., 1986). In its active form the photoprotein includes an apoprotein and a covalently bound prosthetic group, coelenterazine. When calcium ions bind to the three high affinity EF hand sites, coelenterazine is oxidized to coelenteramide, with a concomitant release of carbon dioxide and emission of light.

Although this reaction is irreversible, in vitro an active aequorin can be obtained by incubating the apoprotein with coelenterazine in the presence of oxygen and 2-mercaptoethanol. Reconstitution of an active aequorin (expressed recombinantly) can be obtained also in living cells by simple addition of coelenterazine to the medium. Coelenterazine is highly hydrophobic and has been shown to permeate cell membranes of various cell types, ranging from the slime mold Dictyostelium discoideum to mammalian cells and plants.

Different coelenterazine analogues have been synthesized that confer to the reconstituted protein specific luminescence properties (Shimomura O., 1993). A few synthetic analogues of coelenterazine are now commercially available from Molecular Probes.

The possibility of using aequorin as a calcium indicator is based on the existence of a well characterized relationship between the rate of photon emission and the free Ca^{2+} concentration. For physiological conditions of pH, temperature and ionic strength, this relationship is more than quadratic in the range of $[Ca^{2+}]$ 10^{-5}-10^{-7} M. The presence of 3 Ca^{2+} binding sites in aequorin is

responsible for the high degree of cooperativity, and thus for the steep relationship between photon emission rate and $[Ca^{2+}]$. The $[Ca^{2+}]$ can be calculated from the formula L/L_{max}, where L is the rate of photon emission at any instant during the experiment and L_{max} is the maximal rate of photon emission at saturating $[Ca^{2+}]$. The rate of aequorin luminescence is independent of $[Ca^{2+}]$ at very high ($>10^{-4}$ M) and very low $[Ca^{2+}]$ ($< 10^{-7}$ M). However, as described below in more details, it is possible to expand the range of $[Ca^{2+}]$ that can be monitored with aequorin. Although aequorin luminescence is not influenced either by K^+ or Mg^{2+} (which are the most abundant cations in the intracellular environment and thus the most likely source of interference in physiological experiments) both ions are competitive inhibitors of Ca^{2+} activated luminescence. Aequorin photon emission can be also triggered by Sr^{2+} but its affinity is about 100 fold lower than that of Ca^{2+}, while lanthanides have high affinity for the photoprotein (e.g. are a potential source of artifacts in experiments where they are used to block Ca^{2+} channels). pH was also shown to affect aequorin luminescence but at values below 7. Due to the characteristics described above, experiments with aequorin need to be done in well-controlled conditions of pH and ionic concentrations.

Recombinant aequorins.

For a long time the only reliable way of introducing aequorin into living cells has been that of microinjecting the purified protein. This procedure is time consuming and laborious and requires special care in handling of the purified photoprotein. Alternative approaches (scrape loading, reversible permeabilization, etc.) have been rather unsuccessful. The cloning of the aequorin gene has opened the way to recombinant expression and thus has largely expanded the applications of this tool for investigating Ca^{2+} handling in living cells. In particular, recombinant aequorin can be expressed not only in the cytoplasm, but also in specific cellular locations by including specific targeting sequencing in the engineered cDNAs. Extensive manipulations of the N-terminal of

aequorin have been shown not to alter the chemiluminescence properties of the photoprotein and its Ca^{2+} affinity. On the other hand, even marginal alterations of the C-terminal either abolish luminescence altogether or drastically increase Ca^{2+} independent photon emission. As demonstrated by Watkins and Campbell, the C-terminal proline residue of aequorin is essential for the long-term stability of the bound coelenterazine (Watkins N.J., and Campbell A.K., 1993). For these reasons, all targeted aequorins synthesized in our laboratory include modifications of the photoprotein in the N-terminal. Three targeting strategies have been adopted:

1. Inclusion of a minimal targeting signal sequence to the photoprotein cDNA. This strategy was initially used to design the mitochondrial aequorin and was followed also to synthesize an aequorin localized in the nucleus and in the lumen of the Golgi apparatus.

2. Fusion of the cDNA encoding aequorin to that of a resident protein of the compartments of interest. This approach has been used to engineer aequorins localized in the sarcoplasmic reticulum (SR), in the nucleoplasm and cytoplasm (shuttling between the two compartments depending on the concentration of steroid hormones), on the cytoplasmic surface of the endoplasmic reticulum (ER) and Golgi and in the subplasmalemma cytoplasmic rim.

3. Addition to the aequorin cDNA of sequences encoding for polypeptides that bind to endogenous proteins. This strategy was adopted to localize aequorin in the ER lumen. We routinely included in all the recombinant aequorins the HA1 epitope-tag that facilitates the immunocytochemical localization of the recombinant protein in the cell.

Chimeric aequorin cDNAs

Below we briefly describe the constructs produced in our laboratory. A few other constructs have been produced in other laboratories and will not be dealt with in detail here.

Cytoplasm (cytAEQ)： an unmodified aequorin cDNA encodes a protein that, in mammalian cells is located in the cytoplasm and, given its small size, also diffuses into the nucleus. An alternative

construct is also available that is located on the outer surface of the ER and of the Golgi apparatus. This construct was intended to drive the localization of aequorin to the inner surface of the plasma membrane given that it derives from the fusion of the aequorin cDNA with that encoding a truncated metabotropic glutamate receptor (mgluR1). The encoded chimeric protein, however, remains trapped on the surface of the ER and Golgi apparatus, with the aequorin polypeptide facing the cytoplasmic surface of these organelles. The cytoplasmic signal revealed by this chimeric aequorin is indistinguishable from that of a cytoplasmic aequorin, but it has the advantage of being membrane bound and excluded from the nucleus.

Mitochondria (mtAEQ): mtAEQ was the first targeted aequorin generated in the laboratory, which has been successfully employed to measure [Ca^{2+}] of mitochondrial matrix of various cell types. This construct includes the targeting presequence of subunit VIII of human cytochrome c oxidase fused to the aequorin cDNA.

*Endoplasmic Reticulum (erAEQ):*The erAEQ includes the leader (L), the VDJ and Ch1 domains of an Ig2b heavy chain fused at the N-terminal of aequorin. Retention in the ER depends on the presence of the Ch1 domain that is known to interact with high affinity with the luminal ER protein BiP.

To expand the range of Ca^{2+} sensitivity that can be monitored with the different targeted aequorins we have also employed in many of our constructs a mutated form of the photoprotein (asp119 → ala). This point mutation affects specifically the second EF hand motive of wild type aequorin. The affinity for Ca^{2+} of this mutated aequorin is about 20 fold lower than that of the wild type photoprotein. Chimeric aequorins with the mutated isoform are presently available for the cytoplasm, the mitochondrial matrix, the ER and SR, the Golgi apparatus and the sub-plasmamembrane region.

Cell preparation and transfection

Although in a few cases the aequorin cDNA has been microinjected, the most commonly employed method to obtain expression of the recombinant protein is transfection. Different expression plasmids have been employed, some commercially available (pMT2, pcDNAI and 3) other have been kindly provided by colleagues. The calcium phosphate procedure is by far the simplest and less expensive and it has been used successfully to transfect a number of cell lines, including HeLa, L929, L cells, Cos 7, A7r5 and PC12 cells, as well as primary cultures of neurons and skeletal muscle myotubes. Other transfection procedures have been also employed, such as liposomes, the "gene gun" and electroporation. Viral constructs for some aequorins are also available (Alonso M.T. 1998; Rembold C.M., 1997). In this section we briefly describe the calcium phosphate procedure, a simple and convenient transfection method for HeLa cells.

One day before the transfection step, HeLa cells mantained in Dulbecco Modified Eagle's Medium (DMEM) supplemented with 10% Fetal Bovine serum (FBS) are plated on a 13 mm round coverslip at 30-50% confluence. Just before the transfection procedure, cells are washed with 1 ml of fresh medium.

Calcium-Phosphate transfection procedure

The following stock solutions need to be prepared and conserved at -20°C until used: $CaCl_2$ 2.5 M, HEPES Buffered Solution (HBS): NaCl 280mM, Hepes 50 mM, Na_2HPO_4 1.5 mM, pH 7.12, Tris-EDTA (TE): Trizma-base 10mM, EDTA 1mM, pH 8.

All solutions are sterilized by filtration using 0.22 µm filters. For one coverslip, 5 µl of $CaCl_2$ 2.5 M are added to the DNA dissolved in 45 µl of TE. Routinely, 4 µg of DNA are used to transfect one coverslip. The solution is then mixed under vortex with 50 µl of HBS and incubated for 20 to 30 minutes at room temperature. The cloudy solution is then added directly to the cell monolayer. 18-24 hours after addition of the DNA, cells are washed with PBS (2 or 3 times until the excess

precipitate is completely removed). Using this protocol the transfected cells are usually between 30 and 50 %. Although an optimal transfection is obtained after an overnight incubation, we found that a substantial aequorin expression, sufficient for most experimental conditions, is obtained also with an incubation of only 6 hours with the Ca^{2+}-phosphate-DNA complex.

Reconstitution of functional aequorin

Once expressed, the recombinant aequorin must be reconstituted into the functional photoprotein. This is accomplished by incubating cells with the synthetic coelenterazine for variable periods of time (usually 1-3 hours) and under conditions of temperature and [Ca^{2+}] that depend on the compartment investigated. Practically, coelenterazine is dissolved at 0.5 mM in pure methanol as a 100X stock solution kept at - 80°C. This solution tolerates several freeze-thaw cycles.

However, we recommend the supply of coelenterazine solution to be split into small aliquots (50 µl). Coelenterazine must be protected from light.

For compartments with low [Ca^{2+}] under resting conditions (cytosol and mitochondria) the cells transfected with the appropriate recombinant aequorins are simply incubated at 37°C in fresh DMEM medium supplemented with 1% FBS and 5 µM coelenterazine. Higher or lower coelenterazine concentrations can be also used, if necessary. Good reconstitution is achieved with 1hour incubation, but an optimal reconstitution requires 2 hours.

For compartments endowed with high [Ca^{2+}] under resting conditions (ER), to obtain good reconstitution and interpretable data it is first necessary to reduce the [Ca^{2+}] in the organelle, otherwise aequorin would be immediately consumed after reconstitution and in steady state little functional photoprotein would be present in cells. Depletion of Ca^{2+} from the organelles can be achieved in different ways. Here we describe a simple protocols: cells are incubated at 37°C for 5 minutes in KRB solution (Krebs-Ringer modified buffer: 125 mM NaCl, 5mM KCl, 1mM Na_3PO_4,

1mM $MgSO_4$, 5.5 mM glucose, 20 mM Hepes, pH 7.4) supplemented with 600 µM EGTA, 10 µM ionomycin). After washing with KRB containing 100 µM EGTA and 5% bovine serum albumin, cells are further incubated in the same medium supplemented with 5 µM coelenterazine for 1 hour, but at 4°C.

Slight variations in these depletion protocols have been used both by our group and other investigators. Here it is necessary to stress a few general aspect of the procedure: i) the more efficient the Ca^{2+} depletion, the better the reconstitution; ii) some compartments (e.g. the Golgi and in part the ER) can deeply morphologically altered by the Ca^{2+} depletion protocol. The incubation at 4°C largely prevents these morphological changes, without altering the efficacy of the reconstitution; iii) if ionophores or SERCA inhibitors are employed for depletion they must be removed completely before starting the experiment. For this reason extensive washing of the cell monolayer with Bovine Serum Albumin (BSA) is recommended at the end of the reconstitution procedure.

Luminescence detection

The aequorin detection system is derived from that described by Cobbold and Lee and is based on the use of a low noise photomultiplier placed in close proximity (2-3 mm) of aequorin expressing cells. The cell chamber, which is on the top of a hollow cylinder, is adapted to fit 13-mm diameter coverslip. The volume of the perfusing chamber is kept to a minimum (about 200 µl). The chamber is sealed on the top with a coverslip, held in place with a thin layer of silicon. Cells are continuosly perfused via a peristaltic pump with medium thermostated via a water jacket at 37°C. The photomultiplier (EMI 9789 with amplifier-discriminator) is kept in a dark box and cooled at 4°C.

During manipulations on the cell chamber, the photomultiplier is protected from light by a shutter. During aequorin experiments, the shutter is opened and the chamber with cells is placed in close proximity of the photomultiplier. The output of the amplifier-discriminator is captured by an

EMIC600 photon-counting board in an IBM compatible microcomputer and stored for further analysis.

Ca^{2+} measurement

For the cells transfected with cytosolic, mitochondria or nuclear aequorins, the coverslip with the transfected cells is transferred to the luminometer chamber and it is perfused with KRB saline solution in presence of 1 mM $CaCl_2$ to remove the excess coelenterazine. The stimuli or drugs to test are added to the perfusing medium and reach the cells with a lag time that depends on the rate of the flux and the length of the tubes. In order to make the stimulation more rapid and homogeneous the rate of the peristaltic pump is set to its maximum speed. Under these conditions we calculated that the whole monolayer is homogeneously exposed to the stimuli in 2 sec. At the end of the experiments, all the aequorin is discharged by permeabilizing the cells using a hypotonic solution containing digitonin (100 μM) and $CaCl_2$ (10 mM).

For erAEQ transfected cells, unreacted coelenterazine and drugs are removed by prolonged perfusion (3-6 min) with a saline solution containing 600 μM EGTA and 2% BSA. BSA is then removed from the perfusion buffer and the refilling of the compartments is started by perfusing the medium containing 1mM $CaCl_2$. To note that BSA increases luminescence background level. We found that, despite the depletion protocol and the use of a low Ca^{2+} affinity aequorin mutant, the rate of aequorin consumption upon Ca^{2+} refilling is so rapid that most aequorin is consumed in 30 sec and the calibration of the signal in terms of $[Ca^{2+}]$ becomes unreliable. Two alternative solutions to this problem have been developed, i) the use of Sr^{2+} as a Ca^{2+} surrogate and ii) the reconstitution not with the wild type coelenterazine, but with the analogue coelenterazine n that reduces the rate of aequorin photon emission at high $[Ca^{2+}]$. In the latter case $[Ca^{2+}]$ between 10^{-4} and 10^{-3} M can be reliably calibrated (Robert V., 1998).

Conversion of the luminescent signal into [Ca^{2+}]

To transform luminescence values into [Ca^{2+}] values, we have used the method described by Allen and Blink. The method relies on the relationship between [Ca^{2+}] and the ratio between the light intensity recorded in physiological conditions (L, counts/s) and that which would have been reported if all the aequorin was instantaneously exposed to saturating [Ca^{2+}] (L_{max}). Given that the constant rate of aequorin consumption at saturating [Ca^{2+}] is 1.0 s^{-1}, a good estimate of L_{max} can be obtained from the total aequorin light output recorded from the cells after discharging all the aequorin. This usually requires the addition of excess Ca^{2+} and detergents as shown in the previous section. As aequorin is being consumed continuously, it must be stressed that, for calibration purposes, the value of L_{max} is not constant and decreases steadily during the experiment. The value of L_{max} to be used for [Ca^{2+}] calculations at every time point along the experiment should be calculated as the total light output of the whole experiment minus the light output recorded before that point.

The relationship between the ratio (L/L_{max}) and [Ca^{2+}] has been modeled mathematically.

The model postulates that each of the Ca^{2+} binding sites has two possible states, T and R and that light is emitted when all the sites are in the R state. Ca^{2+} is assumed to bind only in the R state. This model contains three parameters: KR, the Ca^{2+} association constant, KTR= [T]/[R], and n, the number of Ca^{2+} binding sites. The values we obtained for the recombinantly expressed aequorin for each parameter are: KR = 7.23 10^6 M^{-1}, KTR = 120, n=3. The equation for the model provides the algorithm we used to calculate the [Ca^{2+}] values at each point where Ratio is $(L/L_{max})1/n$.

$$Ca^{2+}(M) = \frac{\text{Ratio} + (\text{Ratio} \times KTR) - 1}{KR - (\text{Ratio} \times KR)}$$

Imaging techniques

All imaging experiments were carried out on Zeiss Axiovert 200 inverted microscopes, equipped with cooled CCD digital cameras. Z-series of images were acquired at 0.5 µm distance, deconvolved using a custom-made algorithm and 3D reconstructed as described previously (Carrington W.A., 1995; Rizzuto R., 1998b).

ATP measurements

Luciferase assay was carried out, as previously described. (Jouaville L. S. 1999). In brief, HeLa cells (50,000-70,000 per coverslip) were transfected with mitochondrial targeted luciferase (mtLUC) according to a standard calcium-phosphate procedure.

24 hours after transfection, the coverslip with the cells was transferred to the 37°C termostated chamber of a luminometer and perfused with a Krebs Ringer Buffer containing: 125mM NaCl, 5mM KCl, 1mM Na_3PO_4, 1mM $MgSO_4$, 20µM Luciferin, 20mM Hepes, 5,5 mM Glucose (pH7,4). Luminescence is entirely dependent on the continuosly provided luciferin and proportional to its concentration between 20 and 200 µM. After a preliminary phase of equilibration, during which light emission of mitochondrial luciferase transfected cells was in the range of 14000-16000 cps versus a background lower than 10 cps, cellular response was evoked by the agonist Histamine 100µM added to the perfusion medium.

Subcellular fractionation and proteomic analysis

HeLa cells and mouse liver were homogenized, and crude mitochondrial fraction (8,000g pellet) was obtained. Mouse tissue was subjected to separation on a 30% self-generated Percoll gradient as described previously (Vance J.E., 1990). A low-density band (denoted as MAM fraction) was collected and analysed by immunoblotting. For SDS-PAGE analysis of MAM fraction proteins 10 µg proteins were loaded on 10% SDS-polyacrilamyde gels. The antibodies used were: αIP3R3, isotype

specific monoclonal antibody, 1:1000, Cell Signaling; αVDAC2, 1:1000 Molecular Probe; Smad2/3 monoclonal antibody 1:1000, Cell Signaling, phospho-Smad3 1:1000 monoclonal antibody, Cell Signaling; αActin 1:10000 Cell Signaling; Sigma Receptor 1, 1:1000 monoclonal antibody, Sigma.

The pSUPER RNAi system

In several organisms, introduction of double-stranded RNA has proven to be a powerful tool to suppress gene expression through a process known as RNA interference. However, in most mammalian cells this provokes a strong cytotoxic response. This non-specific effect can be circumvented by use of synthetic short [21- to 22-nucleotide] interfering RNAs (siRNAs), which can mediate strong and specific suppression of gene expression. However, this reduction in gene expression is transient, which severely restricts its applications. To overcome this limitation, the pSUPER RNAi system provides a mammalian expression vector that directs intracellular synthesis of siRNA-like transcripts. The vector uses the polymerase-III H1-RNA gene promoter, as it produces a small RNA transcript lacking a polyadenosine tail and has a well-defined start of transcription and a termination signal consisting of five thymidines in a row (T5). Most important, the cleavage of the transcript at the termination site is after the second uridine, yielding a transcript resembling the ends of synthetic siRNAs, which also contain two 3' overhanging T or U nucleotides. The pSUPER RNAi System has been used to cause efficient and specific down-regulation of gene expression, resulting in functional inactivation of the targeted genes. Stable expression of siRNAs using this vector mediates persistent suppression of gene expression, allowing the analysis of loss-of-function phenotypes that develop over longer periods of time. To effect the silencing of a specific gene, the pSUPER vector is used in concert with a pair of custom oligonucleotides that contain, among other features, a unique 19-nt sequence derived from the mRNA transcript of the gene targeted for suppression (the "N-19 target sequence").

The N-19 target sequence corresponds to the sense strand of the pSUPER-generated siRNA, which in turn corresponds to a 19-nt sequence within the mRNA. In the mechanism of RNAi, the antisense strand of the siRNA duplex hybridizes to this region of the mRNA to mediate cleavage of the molecule. The technical procedure is summarized in the following paragraph.

>> Step One: Anneal Oligos

Two custom DNA oligonucleotides were dissolved in sterile, nuclease-free H_2O to a concentration of 3 mg/ml. The annealing reaction was assembled by mixing 1 µl of each oligo (forward and reverse) with 48 µl annealing buffer (100 mM NaCl and 50 mM HEPES pH 7.4) and incubated at 90°C for 4 minutes, and then at 70°C for 10 minutes. Slowly the annealed oligos were cooled to 10°C.

>> Step Two: Linearize the Vector

1 µl of the pSUPER vector was linearized with Bgl II and Hind III restriction enzymes, then the reaction was heat inactivated (raising the temperature to 65 or 80°C for 20 minutes). Following digestion, purification of the linearized vector, on a 1% agarose gel, was performed to remove the fragment, and to help to separate the prep from any undigested circular plasmid and to decrease the background in ligation and transformation.

>> Step Three: Ligation into pSUPER Vector

For the ligation 2 µl of the annealed oligos, 1µl of T4 DNA ligase buffer, 1µl pSUPER vector, 5µl nuclease-free H_2O, and 1µl T4 DNA ligase were assembled and incubated overnight at room temperature. A negative control cloning reaction was performed with the linearized vector alone and no insert.

>>Step Four: Transformation in Bacteria

Recombinant pSUPER vector was transformed into competent cells. In order to monitor the efficiency of the transformation steps, as a negative control, cells should also be transformed either with a vector that has been ligated with a scrambled-base hairpin oligo, or with a circular vector containing no oligo insert. Bacteria were grown in amp-agarose plates overnight (16-24 hrs), then colonies were chosen for additional cycle in an ampicilin broth. Finally we checked the

presence of positive clones by digesting with EcoRI and Hind III. After digestion, we determine our results as follows:

Positive clone: vector with insert of 281 bp

Negative clone: vector with insert of 227 bp

In addition, the presence of the correct insert within recombinant pSUPER vector was confirmed by sequencing prior to transfection in mammalian cells.

High-throughput assay based on a SiRNAs Library

A custom siRNA library targeting 750 human kinases with three fold redundancy was obtained from Ambion Inc. and the three siRNA duplexes for each target were individually arrayed in 96-well format. A stable clone of HeLa cells overexpressing mitochondrial targeted aequorin probe was exploited. Cells were seeded on 96-well plates at density of 10000 cells per well and cultured overnight at 37°C. 24 hours post-seeding cells were transfected with 50nM siRNA using Lipofectamine 2000 reagent. Forty-eight hours after transfection, thanks to the MicroBeta multiplate reader, cells were challenged with histamine 50µM and mitochondrial calcium transients were measured.

RESULTS

High throughput screen of human kinases for the identification of new regulators of mitochondrial calcium signaling

To establish the role of protein kinases in mitochondrial calcium signaling we designed a functional assay based on RNA interference to perform a genetic screen using small interfering RNA (siRNA) targeting the complete array of human kinases. HeLa cells were systematically co-transfected with the mitochondrially targeted probe aequorin and siRNAs using a kinome library comprising 750 kinases at three fold redundancy. 48 hours post transfection HeLa cells were measured by the multi detector system MicroBeta JET based on the biolumiscent reaction of Aequorin. The aequorin photoprotein undergoes a bioluminescent reaction in the presence of calcium ions, producing a flash of light at 469 nm. This wavelength correlates well with the maximum efficiency of the photo-multiplier tubes used in the MicroBeta.

$$aequorin + Ca^{2+} \rightarrow apoaequorin + coelenteramide + CO_2 + light\ (469nm)$$

The effect of each siRNA was compared with that of a validate one (VDAC2 siRNA) and that of a scrambled sequence, both of them were transfected on each single plate and measured along with the respective samples.

Figure 1

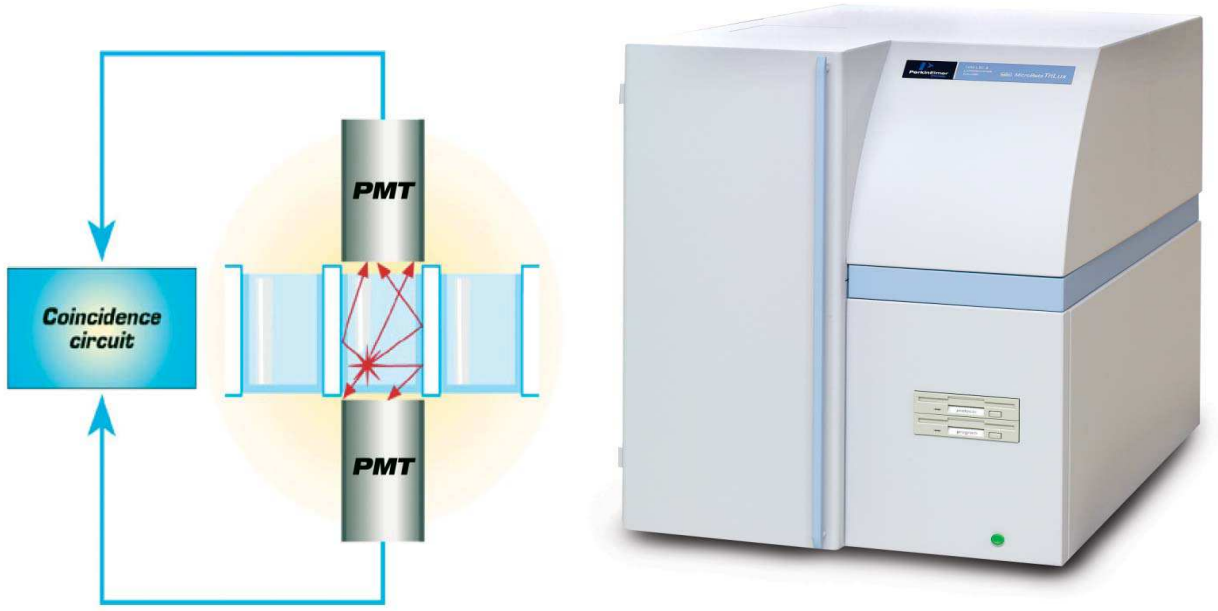

Fig. 1 MicroBeta® JET is a multi-detector instrument designed for liquid scintillation or luminescence detection of samples in microplates, tubes or on filters. MicroBeta JET also includes one or more reagent injectors for measuring prompt (or 'flash') reactions. Multi-detector versions of the instrument can have one or two Injector Modules installed to measure one or two injection and counting sequences.
The single detector MicroBeta JET can have up to four Injector Modules.

Calcium transients were measured in HeLa cells, after reconstitution with the aequorin co-factor coelenterazine, cells were challenged with histamine 100 µM and luminescence was measured and converted in numbers representing the percentage of probe consumption after agonist stimulation, this number was transformed in a percentage of variation of each sample compared to the scrambled siRNA spotted on each plate and Library samples are shown in Table1. Table 1 contains proteins which the three siRNA sequences exert the same effect on mitochondrial calcium uptake, 217 kinases, (28.9% of the entire array) among them the 4.1% shows an increasing in calcium uptake more than 20% while the 37.8% reduces it more than 20% (Fig.2). For 186 (24.8%) human kinases only two siRNA sequences out of three showed consistent effects on mitochondrial calcium signaling, the third one producing no effect at all. The last subgroup of 347

(46.26%) kinases consisted in those with no reproducible effect on calcium transients (data not shown).

Table1

Plate_N°	Row	Col	Symbol	% varsiRNA/scrambled	full_name	locus_link_id
17	B	4	TLK1	-50.7	tousled-like kinase 1	9874
11	C	2	EPHB2	-48.0	EphB2	2048
11	C	1	EPHB1	-43.0	EphB1	2047
11	C	10	FGFR1	-42.4	fibroblast growth factor receptor 1 (fms-related tyrosine kinase 2, Pfeiffer syndrome)	2260
11	B	1	DDR1	-40.5	discoidin domain receptor family, member 1	780
11	H	3	TXK	-40.2	TXK tyrosine kinase	7294
11	B	9	EPHA5	-39.7	EphA5	2044
11	C	4	EPHB4	-39.6	EphB4	2050
4	G	6	C14orf 20	-39.4	chromosome 14 open reading frame 20	283629
9	A	4	STK4	-37.2	serine/threonine kinase 4	6789
11	B	4	EGFR	-36.5	epidermal growth factor receptor (erythroblastic leukemia viral (v-erb-b) oncogene homolog, avian)	1956
12	H	10	ACVRL 1	-36.2	activin A receptor type II-like 1	94
11	H	6	YES1	-36.2	v-yes-1 Yamaguchi sarcoma viral oncogene homolog 1	7525
11	B	11	EPHA8	-35.6	EphA8	2046
9	A	2	STK3	-35.0	serine/threonine kinase 3 (STE20 homolog, yeast)	6788
11	B	7	EPHA3	-34.9	EphA3	2042
11	B	2	DDR2	-34.1	discoidin domain receptor family, member 2	4921
7	B	4	CDKL2	-33.8	cyclin-dependent kinase-like 2 (CDC2-related kinase)	8999
7	C	6	ERK8	-33.7		225689
11	C	5	EPHB6	-33.2	EphB6	2051
9	A	1	STK25	-33.1	serine/threonine kinase 25 (STE20 homolog, yeast)	10494
11	B	6	EPHA2	-32.6	EphA2	1969
17	C	1	PRKW NK3	-31.6	protein kinase, lysine deficient 3	65267
16	G	5	NEK11	-31.4	NIMA (never in mitosis gene a)- related kinase 11	79858
11	B	3	STYK1	-31.3		55359
11	D	4	FLT1	-31.2	fms-related tyrosine kinase 1 (vascular endothelial growth factor/vascular permeability factor receptor)	2321
16	G	1	KIS	-30.3		127933

16	D	7	ASB10	-30.3	ankyrin repeat and SOCS box-containing 10	136371
11	C	9	FER	-30.2	fer (fps/fes related) tyrosine kinase (phosphoprotein NCP94)	2241
4	F	5	CAMK4	-30.2	calcium/calmodulin-dependent protein kinase IV	814
4	F	6	CASK	-29.9	calcium/calmodulin-dependent serine protein kinase (MAGUK family)	8573
17	B	8	ULK1	-29.7	unc-51-like kinase 1 (C. elegans)	8408
11	C	3	EPHB3	-29.6	EphB3	2049
11	C	11	FGFR2	-29.4	fibroblast growth factor receptor 2 (bacteria-expressed kinase, keratinocyte growth factor receptor, craniofacial dysostosis 1, Crouzon syndrome, Pfeiffer syndrome, Jackson-Weiss syndrome)	2263
11	H	8	INSRR	-29.4	insulin receptor-related receptor	3645
7	C	7	HIPK4	-28.9	homeodomain interacting protein kinase 4	147746
16	D	11	TP53RK	-28.9	TP53 regulating kinase	112858
7	B	8	CLK2	-28.8	CDC-like kinase 2	1196
11	H	5	TYRO3	-28.5	TYRO3 protein tyrosine kinase	7301
21	B	3	PKLR	-28.5	pyruvate kinase, liver and RBC	5313
11	B	5	EPHA1	-28.4	EphA1	2041
7	B	6	CDKL5	-28.0	cyclin-dependent kinase-like 5	6792
13	D	1	ZAK	-28.0		51776
7	B	10	CLK4	-28.0	CDC-like kinase 4	57396
8	G	4	MAP3K8	-27.8	mitogen-activated protein kinase kinase kinase 8	1326
11	H	7	FES	-27.4	feline sarcoma oncogene	2242
5	A	5	PRKAA1	-27.3	protein kinase, AMP-activated, alpha 1 catalytic subunit	5562
13	C	1	MAP3K13	-26.8	mitogen-activated protein kinase kinase kinase 13	9175
13	C	2	MAP3K7	-26.7	mitogen-activated protein kinase kinase kinase 7	6885
4	G	5	KIAA1811	-26.3		84446
11	D	10	IGF1R	-26.2	insulin-like growth factor 1 receptor	3480
7	D	1	ICK	-26.1	intestinal cell (MAK-like) kinase	22858
20	D	3	FLJ10842	-26.1		55750
16	H	5	PIK3R4	-25.9	phosphoinositide-3-kinase, regulatory subunit 4, p150	30849
11	D	2	FGFR4	-25.8	fibroblast growth factor receptor 4	2264

7	D	9	MAPK14	-25.1	mitogen-activated protein kinase 14	1432
16	D	9	BUB1	-25.1	BUB1 budding uninhibited by benzimidazoles 1 homolog (yeast)	699
7	B	7	CLK1	-25.0	CDC-like kinase 1	1195
4	H	7	MKNK1	-25.0	MAP kinase interacting serine/threonine kinase 1	8569
26	D	7	T3JAM	-24.7		80342
7	A	8	CDK4	-24.4	cyclin-dependent kinase 4	1019
16	D	6	AAK1	-24.3	AP2 associated kinase 1	22848
4	F	8	CAMK1D	-24.1	calcium/calmodulin-dependent protein kinase ID	57118
4	G	4	KIAA0999	-22.8		23387
20	B	6	CKB	-22.7	creatine kinase, brain	1152
5	B	6	STK17B	-22.4	serine/threonine kinase 17b (apoptosis-inducing)	9262
13	D	3	ANKK1	-22.4	ankyrin repeat and kinase domain containing 1	255239
5	B	7	STK22B	-22.4	serine/threonine kinase 22B (spermiogenesis associated)	23617
5	G	1	CDC2L1	-22.3	cell division cycle 2-like 1 (PITSLRE proteins)	984
21	B	2	PRKD2	-22.2		25865
13	C	3	MFHAS1	-22.1	malignant fibrous histiocytoma amplified sequence 1	9258
16	G	7	NEK3	-22.0	NIMA (never in mitosis gene a)-related kinase 3	4752
13	C	11	TGFBR2	-22.0	transforming growth factor, beta receptor II (70/80kDa)	7048
11	C	8	ERBB4	-21.9	v-erb-a erythroblastic leukemia viral oncogene homolog 4 (avian)	2066
25	C	5	CDKN2D	-21.5	cyclin-dependent kinase inhibitor 2D (p19, inhibits CDK4)	1032
5	B	3	SNRK	-21.4		54861
4	F	2	CAMK2B	-21.4	calcium/calmodulin-dependent protein kinase (CaM kinase) II beta	816
13	C	10	TGFBR1	-21.3	transforming growth factor, beta receptor I (activin A receptor type II-like kinase, 53kDa)	7046
5	A	6	PRKAA2	-21.2	protein kinase, AMP-activated, alpha 2 catalytic subunit	5563
5	C	7	LOC91807	-20.8		91807
11	D	5	FLT3	-20.7	fms-related tyrosine kinase 3	2322
17	B	3	TEX14	-20.0	testis expressed sequence 14	56155
7	B	9	CLK3	-19.8	CDC-like kinase 3	1198
17	A	3	PRKWNK2	-18.4	protein kinase, lysine deficient 2	65268

5	B	8	STK22C	-18.1	serine/threonine kinase 22C (spermiogenesis associated)	81629
5	C	1	TRAD	-17.9		11139
7	D	3	MAK	-17.8	male germ cell-associated kinase	4117
16	H	2	NPR2	-17.2	natriuretic peptide receptor B/guanylate cyclase B (atrionatriuretic peptide receptor B)	4882
16	D	10	BUB1B	-17.1	BUB1 budding uninhibited by benzimidazoles 1 homolog beta (yeast)	701
5	C	4	CHEK1	-16.2	CHK1 checkpoint homolog (S. pombe)	1111
8	E	11	FLJ23074	-16.0		80122
13	C	4	RAF1	-15.2	v-raf-1 murine leukemia viral oncogene homolog 1	5894
5	B	9	STK22D	-14.3	serine/threonine kinase 22D (spermiogenesis associated)	83942
4	E	10	CAMK1	-13.9	calcium/calmodulin-dependent protein kinase I	8536
8	G	2	MAP3K5	-13.2	mitogen-activated protein kinase kinase kinase 5	4217
5	G	5	SCGB2A1	-12.8	secretoglobin, family 2A, member 1	4246
5	F	3	CSNK1G3	-11.9	casein kinase 1, gamma 3	1456
8	G	11	MST4	-11.6		51765
5	F	2	CSNK1G2	-9.8	casein kinase 1, gamma 2	1455
5	F	1	CSNK1G1	-9.5	casein kinase 1, gamma 1	53944
25	C	11	CSNK2B	-9.2	casein kinase 2, beta polipeptide	1460
26	C	9	PRKCDBP	-9.2	protein kinase C, delta binding protein	112464
20	F	9	MGC26597	-9.2		206426
7	A	11	CDK7	-9.0	cyclin-dependent kinase 7 (MO15 homolog, Xenopus laevis, cdk-activating kinase)	1022
20	F	3	ITPKA	-8.6	inositol 1,4,5-trisphosphate 3-kinase A	3706
26	D	4	SKIV2L	-8.6	superkiller viralicidic activity 2-like (S. cerevisiae)	6499
7	D	7	MAPK12	-8.5	mitogen-activated protein kinase 12	6300
14	D	1	BRD2	-8.3	bromodomain containing 2	6046
7	A	10	CDK6	-8.1	cyclin-dependent kinase 6	1021
26	B	6	PKIA	-7.7	protein kinase (cAMP-dependent, catalytic) inhibitor alpha	5569
25	H	1	OSRF	-7.6		23548
13	B	3	IRAK3	-7.6	interleukin-1 receptor-associated kinase 3	11213
21	C	4	SPHK2	-7.5	sphingosine kinase 2	56848
2	D	4	CDC42	-7.4	CDC42 binding protein	9578

			BPB		kinase beta (DMPK-like)	
11	G	6	RYK	-7.2	RYK receptor-like tyrosine kinase	6259
8	F	2	JIK	-7.1		51347
25	G	2	MAPK8IP3	-6.6	mitogen-activated protein kinase 8 interacting protein 3	23162
17	A	1	RNASEL	-6.6	ribonuclease L (2,5-oligoisoadenylate synthetase-dependent)	6041
8	F	3	MAP2K1	-6.3	mitogen-activated protein kinase kinase 1	5604
14	C	11	BCR	-6.0	breakpoint cluster region	613
25	C	7	CIB2	-5.8	calcium and integrin binding family member 2	10518
2	F	8	PKN2	-5.8	protein kinase N2	5586
5	E	9	CSNK1A1	-5.7	casein kinase 1, alpha 1	1452
8	F	1	LYK5	-5.7		92335
11	E	6	KIT	-5.4	v-kit Hardy-Zuckerman 4 feline sarcoma viral oncogene homolog	3815
8	H	2	MYO3B	-5.3	myosin IIIB	140469
12	H	11	ACVR1C	-5.1	activin A receptor, type IC	130399
26	B	2	PIK3R3	-5.1	phosphoinositide-3-kinase, regulatory subunit, polypeptide 3 (p55, gamma)	8503
17	B	6	TOPK	-4.7		55872
13	C	6	RIPK2	-4.7	receptor-interacting serine-threonine kinase 2	8767
8	H	5	PAK2	-4.5	p21 (CDKN1A)-activated kinase 2	5062
7	B	11	CRK7	-4.2		51755
21	B	5	PMVK	-4.1	phosphomevalonate kinase	10654
25	G	1	MAPK8IP2	-4.1	mitogen-activated protein kinase 8 interacting protein 2	23542
2	D	9	GRK5	-4.1	G protein-coupled receptor kinase 5	2869
5	F	8	VRK2	-4.1	vaccinia related kinase 2	7444
20	F	6	KHK	-4.1	ketohexokinase (fructokinase)	3795
14	D	5	CABC1	-4.1	chaperone, ABC1 activity of bc1 complex like (S. pombe)	56997
25	E	9	LOC283846	-3.9		283846
14	D	11	HSPB8	-3.7	heat shock 22kDa protein 8	26353
13	C	7	RIPK3	-3.7	receptor-interacting serine-threonine kinase 3	11035
21	C	9	TPK1	-3.5	thiamin pyrophosphokinase 1	27010
13	B	7	LIMK2	-3.5	LIM domain kinase 2	3985
5	A	10	PSKH1	-3.2	protein serine kinase H1	5681
2	H	8	SGKL	-3.1	serum/glucocorticoid regulated kinase-like	23678
26	B	4	PIP5K1C	-3.1	phosphatidylinositol-4-phosphate 5-kinase, type I,	23396

					gamma	
2	D	8	GRK4	-2.9	G protein-coupled receptor kinase 4	2868
20	F	11	MRC2	-2.9	mannose receptor, C type 2	9902
13	A	2	RIPK4	-2.9	receptor-interacting serine-threonine kinase 4	54101
8	F	6	MAP2K4	-2.8	mitogen-activated protein kinase kinase 4	6416
7	F	2	CDK11	-2.7	cyclin-dependent kinase (CDC2-like) 11	23097
25	C	8	CIB3	-2.7	calcium and integrin binding family member 3	117286
8	H	1	MYO3A	-2.6	myosin IIIA	53904
14	E	11	PRKDC	-2.4	protein kinase, DNA-activated, catalytic polypeptide	5591
20	F	1	IHPK3	-2.4	inositol hexaphosphate kinase 3	117283
25	C	10	CRIM1	-2.3	cysteine-rich motor neuron 1	51232
26	B	3	PIP5K1B	-2.3	phosphatidylinositol-4-phosphate 5-kinase, type I, beta	8395
17	B	5	TLK2	-2.3	tousled-like kinase 2	11011
26	B	5	PIP5KL1	-2.2	phosphatidylinositol-4-phosphate 5-kinase-like 1	138429
14	D	6	EEF2K	-2.1	eukaryotic elongation factor-2 kinase	29904
13	A	3	ARAF1	-2.0	v-raf murine sarcoma 3611 viral oncogene homolog 1	369
20	F	5	ITPKC	-1.9	inositol 1,4,5-trisphosphate 3-kinase C	80271
14	D	4	BRDT	-1.9	bromodomain, testis-specific	676
8	F	4	MAP2K2	-1.7	mitogen-activated protein kinase kinase 2	5605
26	C	7	PRKCABP	-1.4	protein kinase C, alpha binding protein	9463
20	G	2	NAGK	-1.0	N-acetylglucosamine kinase	55577
7	D	11	MAPK6	-0.8	mitogen-activated protein kinase 6	5597
7	E	9	RAGE	-0.6	renal tumor antigen	5891
26	C	5	PRKAR1B	-0.6	protein kinase, cAMP-dependent, regulatory, type I, beta	5575
14	D	10	FRAP1	-0.5	FK506 binding protein 12-rapamycin associated protein 1	2475
2	E	8	PKN3	-0.4	protein kinase N3	29941
4	E	8	TRIB3	0.0	tribbles homolog 3 (Drosophila)	57761
2	F	7	PKN1	0.1	protein kinase N1	5585
20	H	10	PFKFB4	0.2	6-phosphofructo-2-kinase/fructose-2,6-biphosphatase 4	5210
26	A	9	PIK3CD	0.3	phosphoinositide-3-kinase, catalytic, delta polypeptide	5293
26	D	1	SCAP1	0.4	src family associated phosphoprotein 1	8631
20	B	11	DCK	0.5	deoxycytidine kinase	1633

2	E	7	PDPK1	0.7	3-phosphoinositide dependent protein kinase-1	5170
14	D	9	ADCK4	0.8	aarF domain containing kinase 4	79934
7	E	8	PRPF4B	1.0	PRP4 pre-mRNA processing factor 4 homolog B (yeast)	8899
20	D	5	FN3KRP	1.2		79672
26	A	2	PIK3AP1	1.2	phosphoinositide-3-kinase adaptor protein 1	118788
16	E	6	CSNK2A1	1.3	casein kinase 2, alpha 1 polypeptide	1457
21	C	2	RBKS	2.3	Ribokinase	64080
26	C	11	PRKRIR	2.8	protein-kinase, interferon-inducible double stranded RNA dependent inhibitor, repressor of (P58 repressor)	5612
14	E	10	PDK4	3.0	pyruvate dehydrogenase kinase, isoenzyme 4	5166
2	D	7	FLJ25006	3.1		124923
20	D	8	PIP5K2C	3.4	phosphatidylinositol-4-phosphate 5-kinase, type II, gamma	79837
26	B	11	PRKAB2	3.5	protein kinase, AMP-activated, beta 2 non-catalytic subunit	5565
14	D	7	FASTK	3.5		10922
2	F	2	PRKCB1	3.7	protein kinase C, beta 1	5579
20	F	8	LCK	4.3	lymphocyte-specific protein tyrosine kinase	3932
21	A	9	PIP5K1A	4.4	phosphatidylinositol-4-phosphate 5-kinase, type I, alpha	8394
13	A	6	BMPR2	4.5	bone morphogenetic protein receptor, type II (serine/threonine kinase)	659
7	E	11	STK23	4.9	serine/threonine kinase 23	26576
13	A	5	BMPR1B	5.2	bone morphogenetic protein receptor, type IB	658
8	H	7	PAK4	5.9	p21(CDKN1A)-activated kinase 4	10298
14	D	8	RIOK2	6.0	RIO kinase 2 (yeast)	55781
26	D	2	SH3KBP1	6.3	SH3-domain kinase binding protein 1	30011
16	E	7	CSNK2A2	6.5	casein kinase 2, alpha prime polypeptide	1459
13	A	4	BMPR1A	8.7	bone morphogenetic protein receptor, type IA	657
26	D	5	SKP2	8.9	S-phase kinase-associated protein 2 (p45)	6502
20	B	9	CKMT2	9.2	creatine kinase, mitochondrial 2 (sarcomeric)	1160
25	F	8	MAP3K7IP2	11.1	mitogen-activated protein kinase kinase kinase 7 interacting protein 2	23118
2	F	1	PRKCA	11.5	protein kinase C, alpha	5578
25	F	7	MAP3K	15.0	mitogen-activated protein	10454

			7IP1		kinase kinase kinase 7 interacting protein 1	
7	A	5	CDK10	15.8	cyclin-dependent kinase (CDC2-like) 10	8558
25	B	5	AKAP9	31.1	A kinase (PRKA) anchor protein (yotiao) 9	10142
25	B	4	AKAP8L	31.1	A kinase (PRKA) anchor protein 8-like	26993
25	D	11	IHPK2	32.9	inositol hexaphosphate kinase 2	51447
25	B	1	AKAP6	33.2	A kinase (PRKA) anchor protein 6	9472
2	F	4	PRKCE	37.6	protein kinase C, epsilon	5581
25	A	3	AKAP1	46.4	A kinase (PRKA) anchor protein 1	8165
20	E	9	HK2	49.6	hexokinase 2	3099
25	B	8	CALM1	72.9	calmodulin 1 (phosphorylase kinase, delta)	801
25	B	9	CALM2	130.0	calmodulin 2 (phosphorylase kinase, delta)	805

Table1. The table shows 217 kinases which RNAi produce an effect ranging from -50% to 130% on mitochondrial calcium uptake. They are all the mean of the effect of three difference siRNA sequences.

Figure 2

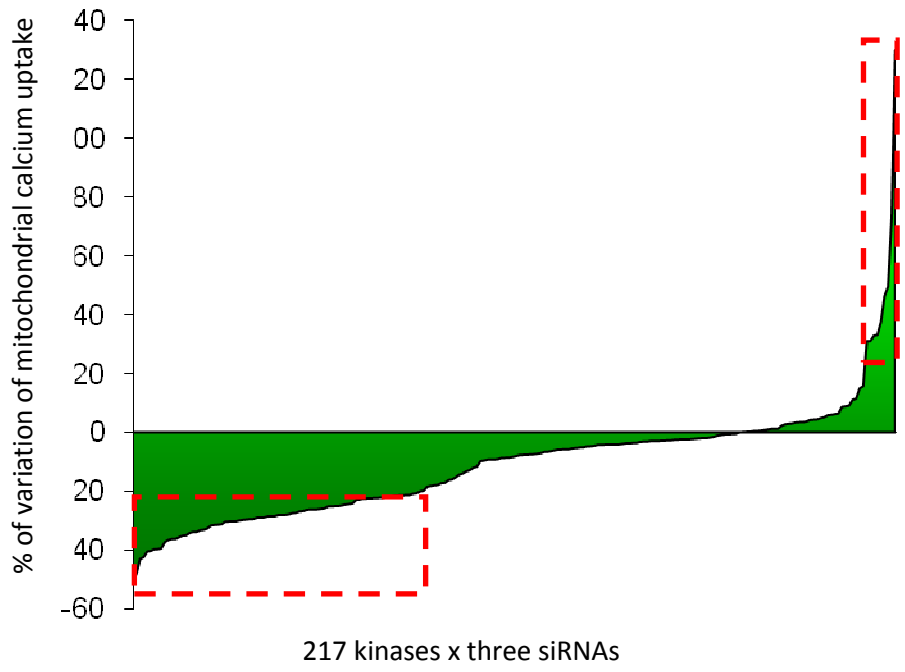

Fig.2 A histogram showing the effect of each kinase (217 kinases with three fold redundancy) on mitochondrial calcium uptake, candidates with average increasing or reducing effect more than 20% are enlightened in red boxes.

According to prior studies Transforming growth factor–β (TGF-β) has been implicated as a key factor in mediating many cellular processes and it has also been demonstrated its ability to impair cytosolic calcium concentration which in some cases may result from the downregulation of the IP_3 receptor Ca^{2+} channels (IP_3Rs). Pieces of evidence collected from many different groups indeed demonstrate that the normal mobilization of intracellular Ca^{2+} stores is reduced in diabetic aortic and proglomerular smooth muscle cells and the alteration is mediated by TGF-β. We decided to concentrate our attention on the study of TGF-β role on mitochondrial calcium uptake and the starting point was coming from the preliminary data collected from the above reported screen which shows that calcium uptake is reduced of 22% by both the isofoms of TGF-β receptor (TGF-βR I and II) .

Mitochondrial Calcium signaling is affected by TGF- β receptor inhibition

The first experiment to be performed was the reproduction of the siRNAs effect on a larger scale. HeLa cells were transfected with the mitochondrially targeted aequorin probe and a reconstituted with the aequorin co-factor coelenterazine; Ca^{2+} transients were trigger by maximal dose of histamine 100μM, luminescence was measured and then converted in $[Ca^{2+}]$. Control coverslips, treated with DMSO, were compared to TGF-β receptor chemical inhibitors SB431542 5μM (inhibitor of TGF-β receptors I and II, signaling mainly through Smad2/3) and Dorsomorphin (DM) 10μM (inhibitor of BMP activated receptors, signaling mainly through Smad1/5/8) treated cells.

The time of treatment was reduced from 16 hours to 4 hours to 10 minutes in order to observe the acute effect on mitochondrial calcium of the chemical silencing of TGF-β receptor signaling cascade. As shown in figure 3A, B and C, the chemical inhibition of TGF-β receptors causes an evident reduction of mitochondrial calcium uptake: while in control cells the mitochondrial

calcium transient observed corresponded to $[Ca^{2+}]_{mt}$ of 128±14.6 µM, after overnight treatment with SB431542 and Dorsomorphin $[Ca^{2+}]_{mt}$ was reduced to 99.5±17.6µM and 72±17.6µM respectively.

Figure 3

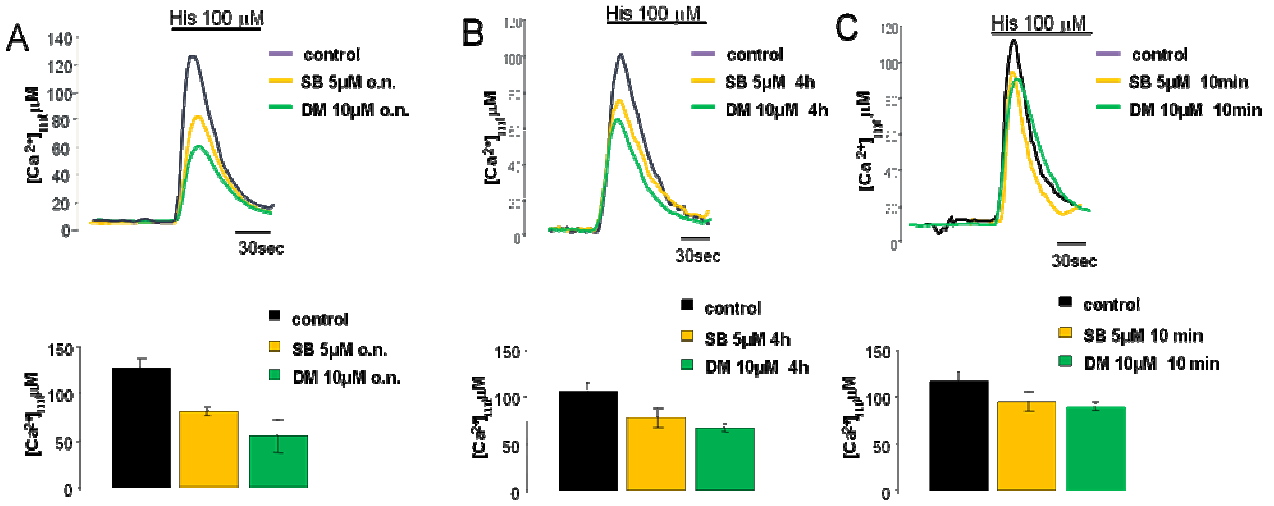

Fig.3 HeLa cells were transfected with mitochondrially-targeted aequorin (mtAEQ). 36 hours after transfection, mitochondrial Ca^{2+} uptake evoked by Histamine 100µM, was measured in three different conditions : A) overnight treatment with SB 431542 (SB) 5µM (inhibitor of TGF-β receptors I and II, signaling mainly through Smad2/3) and Dorsomorphin (DM) 10µM (inhibitor of BMP activated receptors, signaling through Smad1/5/8); B) 4 hours treatment and C) 10 minutes treatment with the same agents. The observed reduction in mitochondrial Ca^{2+} response produced by these treatments was the first indication of a role of TGF-β signalling in the regulation of mitochondrial Ca^{2+} handling.

Thus the effect of two different inhibitors, working on two different subfamily of TGF-β receptor is qualitatively the same, differences in the amplitude of reduction are probably linked to the greater number of inhibited BMP receptors than TGF-β receptors, or differences in receptor affinity to the two chemical compounds.

HeLa cells were transfected with cytosol localizing aequorin Ca^{2+}-probe (CytAeq) and low affinity ER-targeted aequorin based Ca^{2+}-probe, cytosolic and Endoplasmic Reticulum calcium concentration were measured and representative experiments are shown in Fig.4. These results excluded that the mitochondrial calcium uptake reduction observed could be explained by general Ca^{2+} handling impairment nor by defective storing within the major intracellular calcium store,

since no significant difference has been recorded in the two compartments. These data strongly supported the hypothesis of a direct activity of TGF-β on mitochondria while the homeostasis of this ion in the other compartment remained affected.

Figure 4

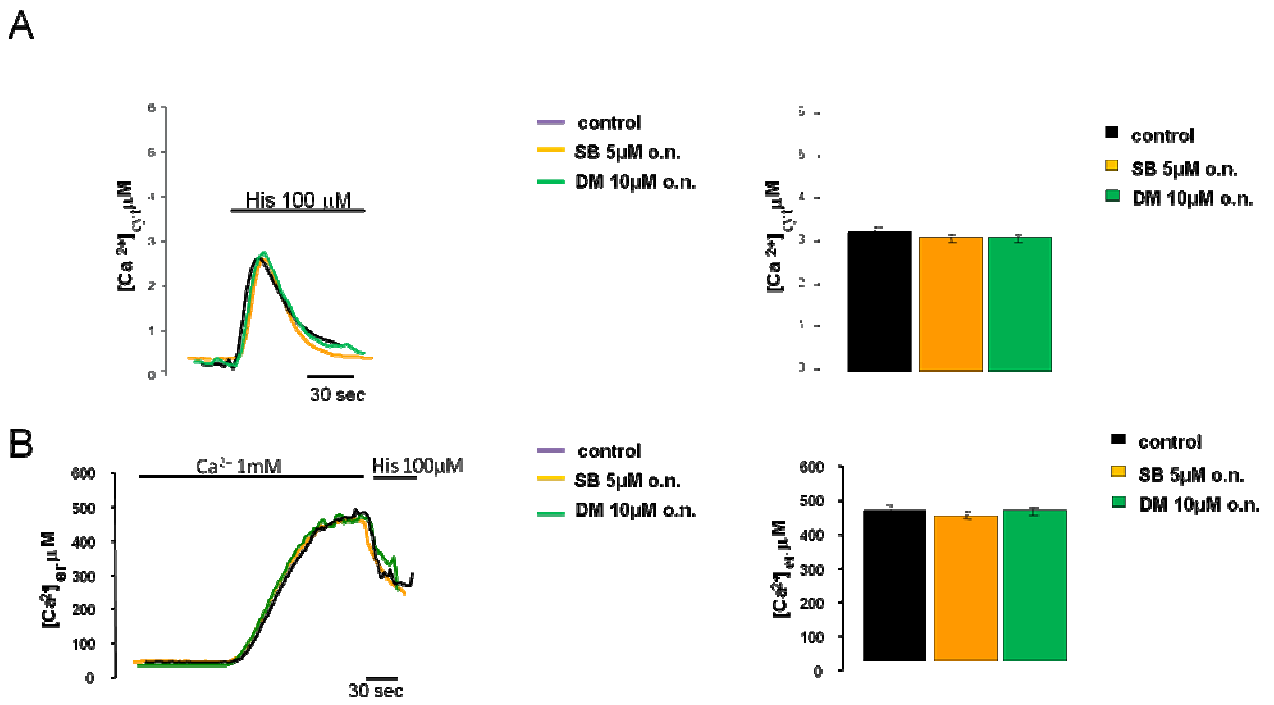

Fig.4 ER and cytosolic Ca^{2+} measurements with targeted aequorin probes. In both compartments, pretreatment with SB and DM did not modify either the resting values nor the peak (cytosol) or decrease (ER) caused by stimulation with Histamine 100µM.

Mitochondrial membrane potential ($\Delta\psi_{mt}$) was measured in HeLa cells in order to test whether mitochondrial calcium uptake reduction is dependent from mitochondrial respiratory chain activity. In living cells $\Delta\psi_{mt}$ was measured using tetramethyl rhodamine methyl ester (TMRM), a fluorescent lipophilic cation that accumulates in the mitochondrial matrix in a $\Delta\psi_{mt}$-dependent way. The fluorescence intensity of TMRM in individual cell was measured using laser scanning microscopy. To measure and compare the potential-dependent staining of TMRM of different conditions, cells were incubated with 1 µM FCCP, a protonophore that collapses the $\Delta\psi_{mt}$. The loss of TMRM fluorescence was used to obtain quantitative analysis of $\Delta\psi_{mt}$. The representative traces

in fig. 5 showed that overnight treatments with SB 5µM and DM 10 µM strongly reduced TMRM fluorescence basal level (-35 ± 8.2% and -42 ± 12.7%) if compared with untreated controls. Since it is well established the notion that $\Delta\psi_{mt}$ drives mitochondrial uptake of Ca^{2+}, these results appeared to be consistent with the previous observation about the mitochondrial calcium uptake impairment, obtained with aequorin measurements after TGF-β receptors inhibition.

Figure 5

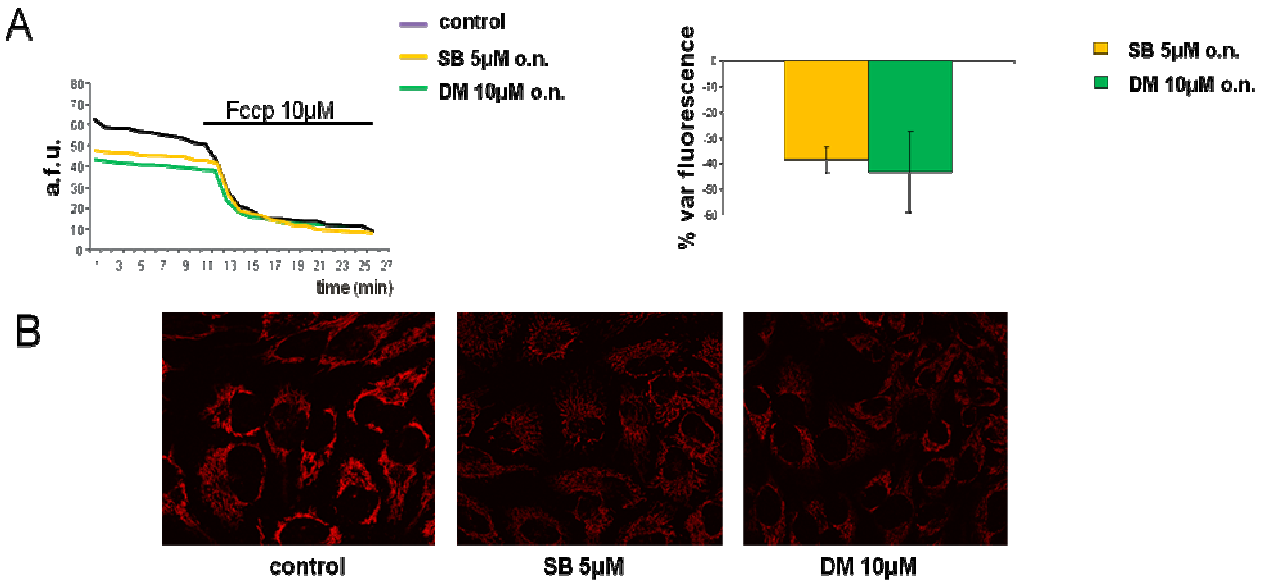

Fig.5 The electrical potential across the mitochondrial inner membrane ($\Delta\psi_{mt}$) was measured with Tetramethyl Rhodamine Methil Ester (TMRM). Mitochondrial TMRM loading at the steady state was significatively decreased by overnight treatment with SB 5µM and DM 10 µM (A, left representative traces; right, quantification in the whole array of analyzed cells). Upon treatment with FCCP, all traces reached the same background level. Figure B shows representative images of HeLa cells incubated with TMRM 10nM for 20 minutes and DMSO, SB 5µM and DM 10µM, fluorescent intesity of TMRM was detected with laser scanning microscopy.

Along the same line were the measurements of mitochondrial ATP production carried out by means of ATP luciferase probe targeted to the mitochondrial compartment. The method is based on the reaction of luciferase with the substrate luciferin in presence of oxygen, being the following light emission a linear function of ATP concentration in a range between 10^{-3} and 10^{-2} M. HeLa cells were transfected with mitochondrial targeted luciferase (mtLUC) and 24 later coverslips were transferred to the 37°C termostated chamber of a luminometer and perfused with a Krebs Ringer Buffer containing 20µM Luciferin. During the preliminary phase of equilibration, light

emission was in the range of 12000-17000 cps versus a background lower than 10 cps, cellular response was evoked by the agonist Histamine 100µM added to the perfusion medium. As previously reported (Jouaville L.S., 1999), agonist-dependent [Ca^{2+}] increases in the mitochondrial matrix cause an increase in ATP levels, both in the mitochondria (Fig.6) and in the cytosol (data not shown). This was mainly attributed to the stimulation of Ca^{2+}-dependent dehydrogenases. We evaluated the effect on level of ATP production produced by acute treatment of HeLa cells with SB 5µM and DM 10 µM. In treated cells, in agreement with our previous results on calcium signaling, ATP production is drastically reduced (fig.6). The impairment of calcium uptake occurring in the organelle after TGF-β receptors inhibition correlates with a minor Ca^{2+}-mediated stimulation of matrix dehidrogenases which leads to the reduction of ATP synthesis observed (-42.8±4.2% for SB and -37.1±6.1% for DM).

Figure 6

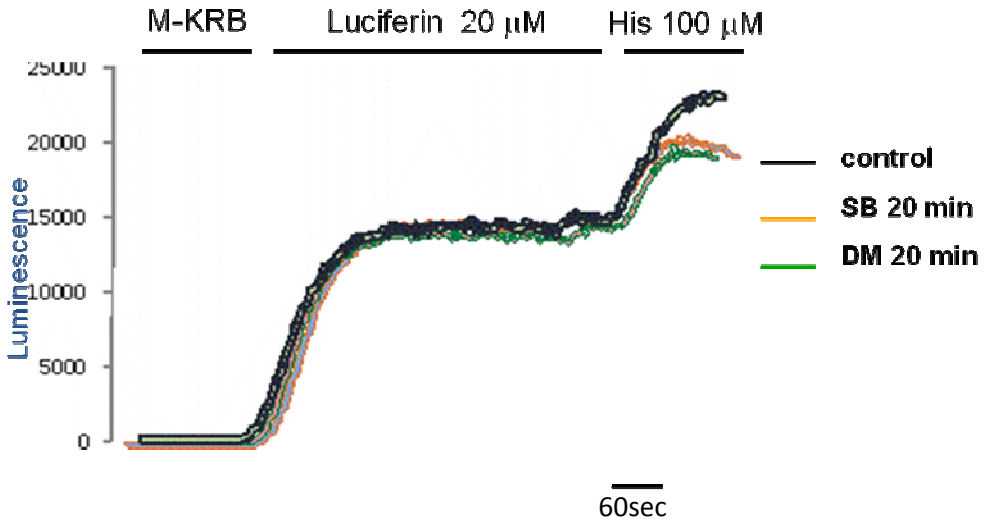

Fig.6 A mitochondrially targeted chimera of ATP-sensitive photoprotein Luciferase (mtLUC) was exploited to dynamically monitore ATP synthesis within the mitochondrial subcellular compartment. HeLa cells were seeded on coverslips and grown in DMEM plus 10% FBS. Two days before the ATP measurements, the two groups of cells were transfected with mtLUC probe, the following day one set of coverslips was treated with dmso (controls), one set with SB 5µM and one set with DM 10uM. For the measurements, the cells were rinsed twice with KRB, then transferred to the luminometer chamber and perfused with KRB supplemented with glucose 5,5mM, calcium 1mM and Luciferin 20µM. 60 seconds were allowed for equilibration in the new medium, then ATP production was triggered by supplementing the perfusion buffer with Histamine 100µM. In presence of TGF-β receptors inhibitors ATP production appeared to be reduce of -42.8±4.2% in the case of SB and of 37.1±6.1% for DM.

TGF-β receptors silencing by means of specific siRNA plasmids

Mitochondrial network and the biophysical properties of mitochondrial calcium uptake have been studied in detail and since it has been demonstrated its high sensitivity to lipholic molecules. In order to evaluate the real effect of TGF-β receptors inhibition, without the usage of chemical compounds dissolved into DMSO, we decided to built up siRNA plasmids to downregulate TGF-β receptor isoforms through RNA interference techniques, so doing we would get rid of any possible non-specific effect due to chemical treatment. Two different sequences for TGF-β receptor I and II were cloned into pSuper Vector (siRNA TGF-βRI and siRNA TGF-βRII) and the silencing capacity of the two most efficient plasmids, chosen for further experiments, is shown in figure 7.

Figure 7

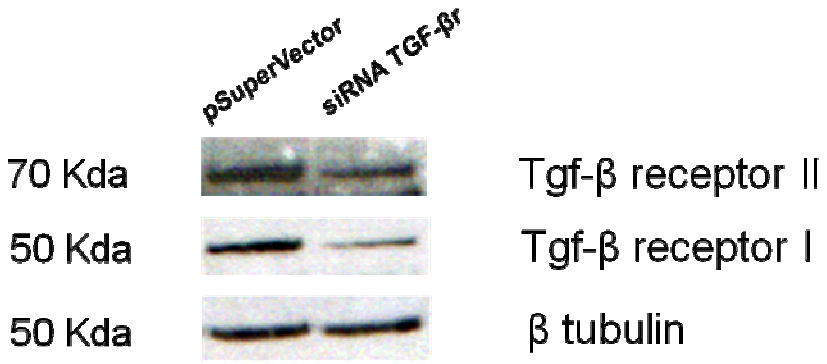

Fig.7 HeLa cells were transfected with small interfering (siRNA) plasmids created using a pSuper vector. We obtained two different sequences cloned in the expression vector, efficently silencing target genes of TGF-β receptor I and II. The western blot shows the most effective sequences we used to perform the following experiments.

Intracellular calcium homeostasis was then analized in HeLa cells after co-transfection of TGF-BR I and II siRNAs and aequorin probes specifically targeted to mitochondria, Endoplasmic Reticulum and cytosol.

The effect is reported in the panel below (fig. 8), where it is evident the peculiar reduction of mitochondrial Ca^{2+} uptake while the other two compartment appeared to be unaffected.

Figure 8

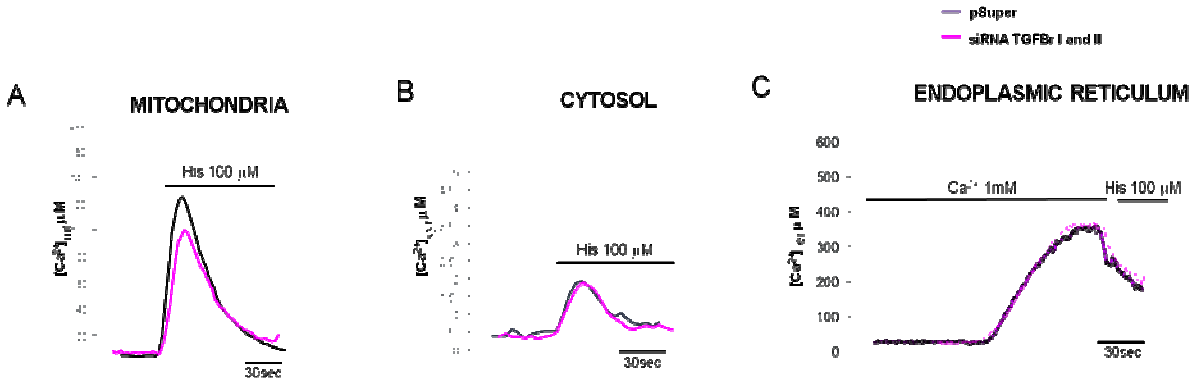

Fig.8 Calcium measurements were carried out in HeLa cells co-transfected with the siRNAs of the two different isoforms of TGF-β receptor and aequorin-based Ca^{2+} probes. The data confirmed that mitochondrial Ca^{2+} response after stimulation was significantly decreased upon suppression of TGF-β signaling, whereas cytosolic and ER Ca^{2+} handling was unaffected.

Mitochondrial membrane potential ($\Delta\psi_{mt}$) was measured in presence of DMSO (as negative control, black line), SB 5µM (as positive control, orange line) and after 36 hours co-transfection with the siRNA plasmids of the two different isoforms of TGF-β receptor.

Comparing the effect exerted by two different tools to achieve TGF-β pathway inactivation, we could assess that they were both on the same line of what had been observed by aequorin measurements, $\Delta\psi_{mt}$ was strongly reduced and mitochondrial Ca^{2+} uptake along with it. (Fig. 9)

Fig. 9

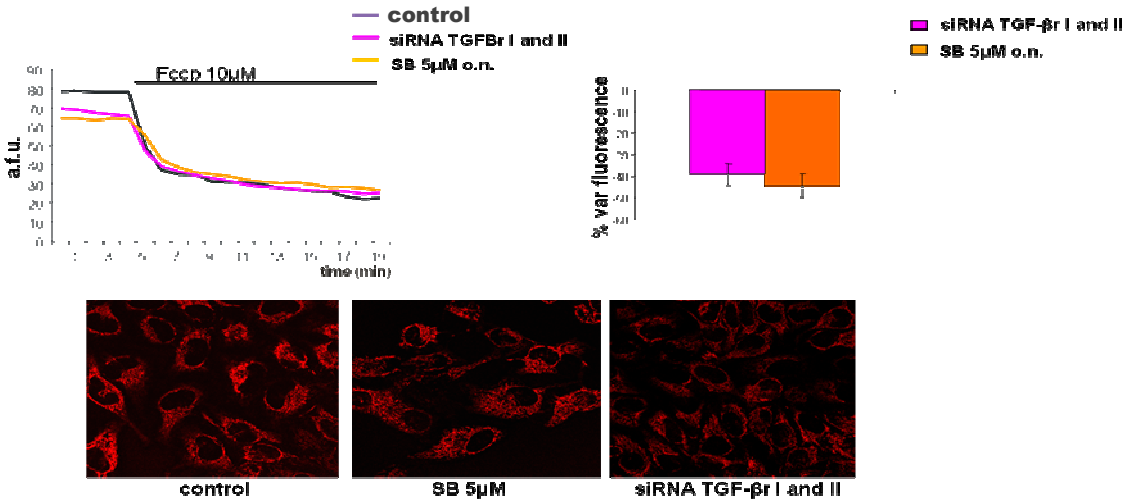

Fig. 9 Mitochondrial membranepotential ($\Delta\psi_{mt}$) was measured with TMRM in untreated HeLa cells (black trace) or after TGF-β receptor inhibition by means of SB 5µM (orange line) or siRNA silencing (pink line).

The effect on mitochondrial Ca^{2+} uptake was thus confirmed by direct specific intraorganelle measurements thanks to aequorin probes, indirectly exploting Luciferase probe specifically targeted to mitochondrial which measured ATP production and finally through TMRM analysis of potential across the mitochondrial membrane.

Subcellular distribution of Smad proteins

The question we had to answer then was: which was molecular mechanism ruling the effect ?

Looking for possible molecular characters we decided to define subcellular localization of TGF-β downstream effectors: the Smad proteins.

Among the huge family of these intracellular transducers we focused our attention on isoforms 2 and 3 because from previous work (Jullig M., 2003) they were demonstrated to be the members with higher mitochondrial distribution.

Mitochondrial cellular fractioning was performed as described in Materials and Methods on HeLa cells to compare Smads localization in mito crude fraction with or without TGF-β receptors inactivation by means of SB treatment.

As it is shown in fig. 10 Smad2/3 was observed in mito crude of HeLa cells, interestingly its phosphorylated fraction appeared to be delocalized from mitochondria after the treatment applied.

Figure 10

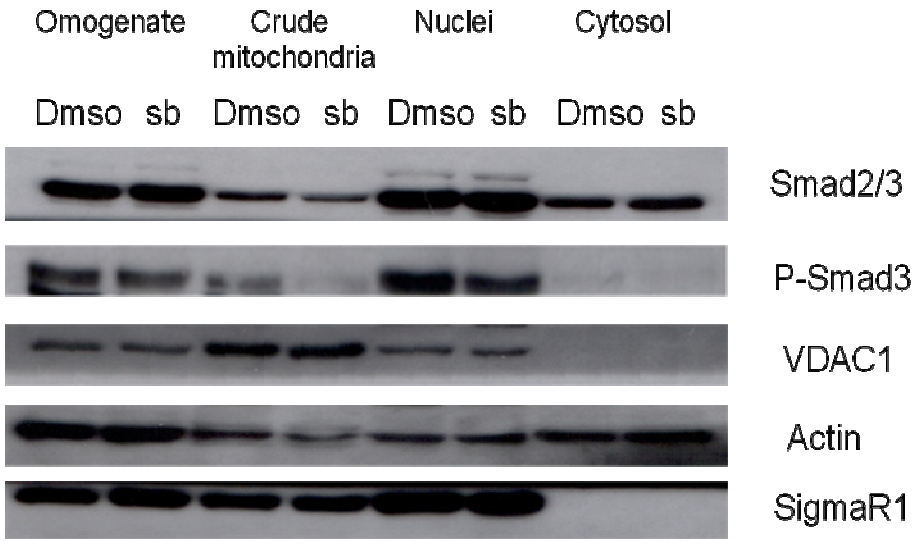

Fig.10 Subcellular localization of Smad proteins, TGF-β receptor effectors. Western blots of subcellular fractions shows mitochondrial distribution of Smad2/3 that was decreased by SB 5μM treatment. Interestingly, we observed the almost complete absence of the phosphorylated protein in mitochondria of HeLa cells treated with the inhibitor.

We thus speculated that most likely the equilibrium between the phosphorylated and unphosphorylated fraction of Smad2/3 could be linked to those mitochondrial events produced by chemical or biological inhibition of TGF-β receptors, described before.

If the mitochondrial delocalization of the specific isoform of Smad proteins was responsible for the impairment of mitochondrial functionality, then the question was: what about the biological mechanism?

Two different possibilities could be envisioned.

In the first one the phosphorylated pool of Smad could act favouring calcium transfer between the major intracellular store, the Endoplasmic Reticulum and mitochondria, thus we measure calcium transient by means of mitochondrial aequorin probe in presence of TGF-β or not. What we observed is shown in figure 11, and despite what was expected, no increase has been recorded in mitochondrial calcium uptake.

Figure 11

A B

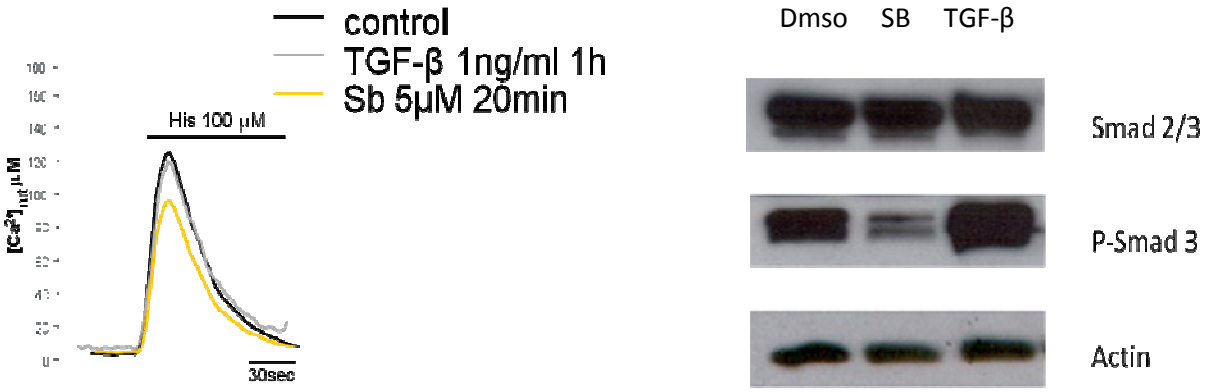

Fig. 11 A) Mitochondrial calcium transients were measured in HeLa cells in presence of TGF-β (1h 1ng/ml), SB (5 μM 20min) or not. Since no significative difference was observed comparing control coverslips and TGF-β treated ones (control 120± 5.4μM, TGF-β 118±6.7 μM, SB 88± 2.4μM) we could asses that increasing the phosphorylated fraction of Smad proteins can not be considered responsible for mitochondrial calcium uptake regulation. B) Western Blot analysis of Smad2/3 and Phospho-Smad3 levels In presence of the same two treatments applied for calcium measurements

In the second scenario, we speculated that the unphosphorylated fraction of Smads could be the true character behind the mitochondrial effect. Indeed inhibiting the plasma membrane receptors by chemical treatments or SiRNA plasmid, the unphosphorylated protein would accumulate and the mitochondrial fraction would increase as a consequence. Therefore if it was true that accumulation of Smads at the mitochondria negatively regulates calcium uptake, inhibiting regular gene expression of Smad proteins by means of specific SiRNA duplexes would revert the effect observed treating HeLa cells with TGF-β receptors inhibitor. Thus we co-transfected HeLa cells with ShRNA of Smad2/3 and Smad4 and mitochondrial aequorin probe in order to measure calcium transients after agonist stimulation. The data collected are shown in figure 12 and as expected mitochondrial calcium uptake is clearly increased where Smad proteins have been silenced.

Figure 12

A B

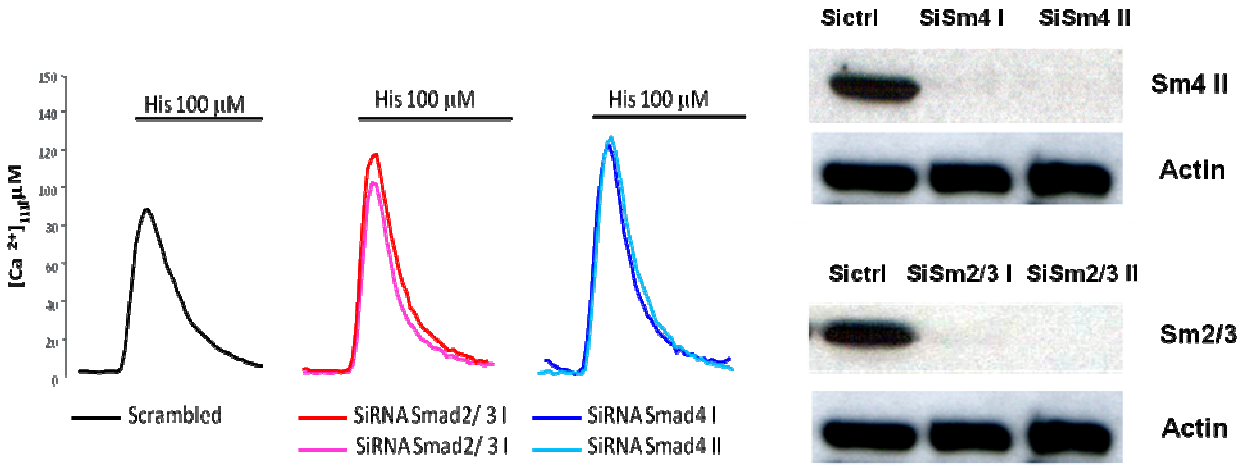

Fig.12 A) Mitochondrial calcium transients were measured in HeLa cells co-transfected with two different ShRNAs of Smad2/3 or Smad4, and mitochondrial aequorin. As shown in panel A silencing Smad proteins enhances mitochondrial calcium uptake. (Scrambled 82± 6.1µM, SiRNA Smad2/3 I 113± 7.2µM, SiRNA Smad2/3 II 120± 4.2µM, SiRNA Smad4 I 121± 9.2µM, SiRNA Smad4 II 125± 6.2µM). B) Western Blot analysis of Smad2/3 and Smad4 levels In presence of their specific ShRNAs.

At this point, the study of a more physiological system than HeLa cells was fundamental, for this reason we wanted to analyze intracellular Smads distribution in mouse liver.

Recently a very accurate method has been described by Wieckowsky and coworkers to obtain mitochondrial purification from different animal tissues by gradient centrifugation in order to separate pure mitochondria from the so called “mitochondria-associated membrane” (MAM) (fig. 13) (Wieckowsky M., 2009). Intriguingly this fraction would prove to be not only mere contamination of pure mitochondria but also a very interesting mitochondrial subfraction, indeed since 1990 the specific mitochondrial regions showing close proximity to the ER cisternae were referred as MAMs by Vance et al. (Vance J.E., 1990). Although they have been firstly described as the headquarters of lipid transfer, today it is widely accepted the notion that MAMs are also involved in rapid movement of Ca^{2+} ions between ER and mitochondria. So doing they play a fundamental role in the coordination of ATP production through the activation of mitochondrial dehydrogenase as well as the activation of the cell death program (Berridge M.J., 2002). The

shaping of the ER-mitochondrial network can be affected by bounding proteins and physiological ligands indeed recently Hajnoczky and coworkers demonstrated that exposure to TGFβ affects Ca^{2+} transfer to the mitochondria (Hajnoczky G., 2008).

Figure 13

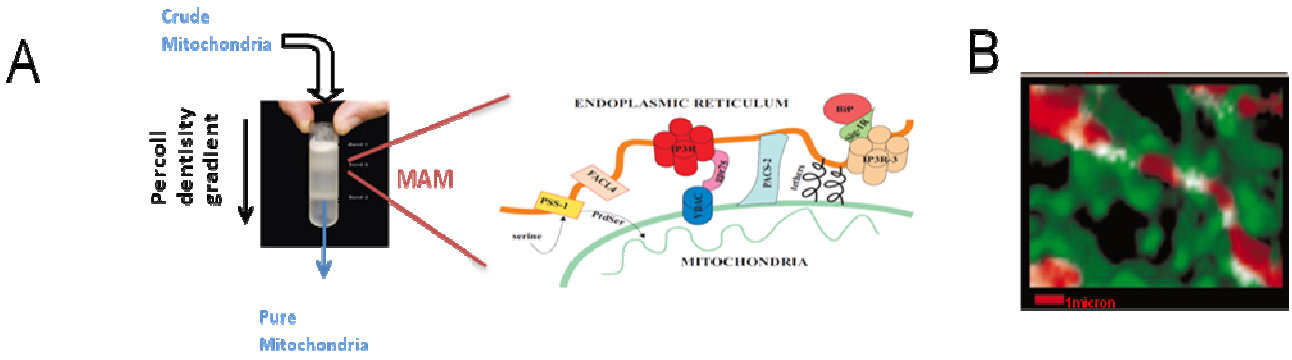

Fig. 13 A) Isolation of Mitochondria Associated Membranes (MAMs) from animal tissues and cells (Wieckowsky M., 2009) B) Combined 3D imaging of mitochondria and ER in a HeLa cell transiently expressing mtGFP(Y66H,Y145F) and erGFP(S65T). The two 3D images were processed and superimposed. The mitochondrial and ER images are represented in red and green, respectively;
the overlaps of the two images are white and constitute the microdomains called MAMs. (Rizzuto R., 1998)

Mouse liver were homogenized, and crude mitochondrial fraction (8,000g pellet) was subjected to separation on a 30% self-generated Percoll gradient as described previously (Vance J.E., 1990). A low-density band (denoted as MAM fraction, fig.14A) was collected and analysed by immunoblotting.

Specific markers were chosen for each different fraction (IP_3 Receptor 3 for MAM and ER fractions, VDAC2 for pure and crude mitochondria, Sigma1 Receptor for MAM and β-actin as cytosolic protein, see figure 14), and from prelimary results Smad2/3 appeared to be clearly localized in the mitochondria and in particular into the MAM fraction.

Figure 14

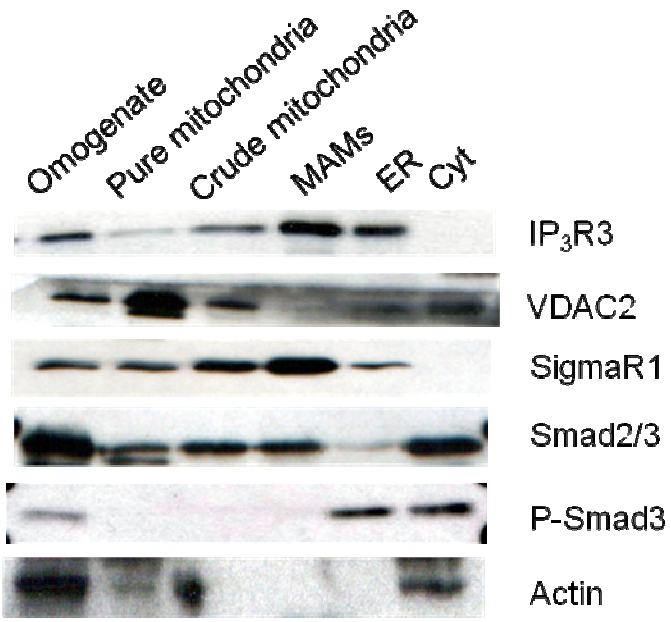

Fig.14 A more extensive subcellular fractionation in mouse liver shows the presence of Smads in the MAM fraction, thus suggesting a direct regulatory role exerted in this signaling domain.

The evidence of Smad2/3 presence in the MAMs obtained from a physiological system such as mouse liver, is the starting point of a wide work that would lead to the understandment of a new role of TGF-β signaling pathway in the orchestration of mitochondrial calcium signaling.

Next step would be the analysis of Smads and phospho-Smads delocalization in vivo after TGF-β receptor inhibition or activation by means of mouse liver perfusion techniques carried out in presence of chemical compounds. Moreover it would be necessary the research of Smads molecular interactors by means of co-immunoprecipitation and Blue Native assays.

Hence, further study will be done to assess a possible direct mitochondrial activity of Smad proteins on the organelle calcium homeostasis.

DISCUSSION

Preliminary results obtained by a screening based on a human kinases library, showed that silencing TGF-β Receptors by means of siRNA duplexes, exerted a clear effect on mitochondrial calcium homeostasis. This starting information was then exploited to unravel the molecular mechanism by which mitochondria could orchestrate intracellular calcium homeostasis.

TGF-β signaling has been widely studied and although its transcriptional activity is today well understood, less efforts have been made to investigate its non-nuclear functions which are still quite unknown.

We thus decided to go deeply through this study, since according to previous works a transcriptional-independent activity of TGF-β cascade had already been observed. First of all, many different groups are engaged in the study of TGF-β role in the regulation of the intrinsic pathway leading to apoptosis. Gottfried in 2004 demonstrated TGF-β activation of ARTS, a proapoptotic protein localized in the mitochondria. Wang et al., in 2008 published the observation that TGF-β treatment could generate reactive oxygen species (ROS) and mitochondrial membrane potential loss in epithelial cell.

Concerning calcium homeostasis, recent works showed that TGF-β could reduce IP_3 Receptor 1 calcium release from ER in diabetic aortic and proglomerular smooth muscle cells.

The first step we took, was to obtain a more complete scenario about intracellular calcium homeostasis after TGF-β signaling inhibition. Overexpressing aequorin probe in HeLa cells, we observed that mitochondrial calcium uptake was impaired when TGF-β signaling was inhibited by

chemical treatments, whereas Endoplasmic Reticulum and cytosolic calcium handling was unaffected.

The same scenario was there inhibiting TGF-β signaling both by molecular inhibitors acute treatment and by transfecting TGF-β receptor siRNA plasmids into the cells.

Mitochondrial functionality was consistently affected in the same conditions, since we observed the reduction of mitochondrial membrane potential and also the ATP production resulted significantly impaired.

Then we focused on how this effect was achieved.

The biochemical meaning of TGF-β receptors inhibition is the reduction of the phosphorylated fraction of TGF-β receptors downstream effectors: the Smad proteins. Therefore we speculated that the mitochondrial specific effect could be the result of two different situation.

According to the first one, reduction of Smad phosphorylation could be direct source of the mitochondrial effect, under the hypothesis that the phosphorylated Smad could positively control calcium transfer between the ER and mitochondrial. Thus we hypothesized that the less is the amount of phospho-Smad working at the mitochondria, the less these organelles are exposed to high Ca^{2+} concentration generated at the mouth of IP_3Rs. As described in the introduction of this work, this could explain the reduction in mitochondrial calcium transient after agonist stimulation.

The second hypothesis envisioned the non-phosphorylated fraction of Smad proteins as responsible for a negative regulation of ER-mitochondrial contacts. Indeed switching off TGF-β receptors avtivity, the intracellular amount of non-pshorylated Smads increased and consequently the equilibrium between the nuclear and mitochondrial (and cytosolic) pools of these proteins, most likely would shift toward the mitochondrial translocation. Blocking TGF-β receptors activity a

great amount of Smad would be potentially disposable for mitochondrial accumulation where it exerted a specific effect on calcium transients.

We thus decided to silence, by means of short hairpin RNA interference, the total amount of specific isoforms of Smads, we chose to silence Smad 2/3 and Smad 4, members of a great family of nuclear factors, which are described to be localized into the mitochondria (which was confirmed in our lab also). So thanks to Smad2/3 and Smad4 shSiRNAs, we measured calcium transients in HeLa cells and we observed a clear augmentation in mitochondrial calcium uptake in coverslips where normal transcription of Smad proteins was blocked, compared to scrambled controls. This observation supported the second hypothesis : the non phosphorylated Smads exerted negative regulation on ER-mitochondrial transfer.

On the other hand, we treated HeLa cells with TGF-β polypeptide and measured mitochondrial calcium uptake. If the first hypothesis had been true, the potentiation of TGF-β receptors activity would have increased the phosphorylation of Smad proteins and consequently the mitochondrial impairment described so far would have had to be inverted. Indeed if phospho-Smad was a positive regulator of mitochondrial function, in TGF-β treated coverslips we should have observed a mitochondrial calcium uptake enhancement.

However no increase was recorded to further support the idea that it was not the phosphorylated but the non-phosphorylated pool of Smads which was responsible for a negative control of ER-mitochondria contacts.

Moreover subcellular fractionation obtained from mouse liver, showed that a good fraction of Smad2/3 protein is localized in the MAM, the well described contact sites between ER and mitochondria.

Although the molecular mechanism that controls different distribution of Smads are still completely unknown (apart from the classical pathway ruling gene transcription) according to our data, a new role for these proteins has been demonstrated, which is independent from the nucleus whereas it appears to be associated to the mitochondria.

Aequorin probe measurements, carried out in living cells, revealed a clear engagement of TGF-β in regulating mitochondrial calcium transient evoked by agonists stimulation.

Moreover biochemical studies demonstrated that there is a specific localization of Smad proteins both in crude mitochondrial fraction and in the low density mitochondrial associated membranes (MAMs) where, most likely, they could participate in complexes with other signaling partners.

In conclusion this work highlights a quite unexplored signaling pathway for TGF-β, telling that Smad proteins can directly regulate mitochondrial calcium homeostasis.

Although much remains to be unraveled, the notion that mitochondrial function could be modulated by highly specialized domains at the ER-mitochondria interface is today generally accepted. More and more efforts will be made in future and other experimental work will be necessary to make it completely understood, so doing novel possibilities will be opened to modulate downstream pathological conditions linked to cellular proliferation or metabolism.

REFERENCES

Alonso M.T., Barrero M.J., Carnicero, E. Montero M., Garcia-Sancho J., and Alvarez J. (1998). Functional measurements of [Ca^{2+}] in the endoplasmic reticulum using a herpes virus to deliver targeted aequorin. Cell Calcium *24*, 87-96.

Berridge MJ. (2002) The endoplasmic reticulum: a multifunctional signaling organelle. Cell Calcium. *32*(5-6):235-49.

Berridge M.J., Bootman M.D., and Roderick H.L. (2003). Calcium signaling: dynamics, homeostasis and remodelling. Nat. Rev. Mol. Cell. Biol. *4*, 517-529.

Bertolino M., and Llinas R.R. (1992). The central role of voltage-activated and receptor-operated calcium channels in neuronal cells. Annu. Rev. Pharmacol. Toxicol. *32*, 399-421.

Carrington W.A., Lynch R.M., Moore E.D., Isenberg G., Fogarty K.E., and Fay F.S. (1995). Superresolution three-dimensional images of fluorescence in cells with minimal light exposure. Science *268*, 1483-1487.

Clybouw C., Mchichi B.E., Hadji A., Portier A., Auffredou M.T., Arnoult D., Leca G., and Vazquez A. (2008). TGFbeta-mediated apoptosis of Burkitt's lymphoma BL41 cells is associated with the relocation of mitochondrial Bim. Oncogene. *29,* 27 (24) 3446-56.

Colombini M. (2004). VDAC: the channel at the interface between mitochondria and the cytosol. Mol Cell Biochem *256-257*, 107-115.

Csordas G., Renken C., Varnai P., Walter L., Weaver D., Buttle K.F., Balla T., Mannella C.A., and Hajnoczky G. (2006). Structural and functional features and significance of the physical linkage between ER and mitochondria. J. Cell. Biol. *174*, 915-921.

Franze´n P., Ten Dijke P., Ichijo H., Yamashita H., Schulz P., and Heldin C-H. (1993). Cloning of a TGF beta type I receptor that forms a heteromeric complex with the TGF beta type II receptor. Cell *75*, 681– 92.

Gottfried Y., Voldavsky E., Yodko L., Sabo E., Ben-Itzhak O., and Larisch S. (2004). Expression of the pro-apoptotic protein ARTS in astrocytic tumors: correlation with malignancy grade and survival rate. Cancer. *101* 11 2614-21

Gunter T.E., Buntinas L., Sparagna G.C., and Gunter K.K. (1998). The Ca^{2+} transport mechanisms of mitochondria and Ca^{2+} uptake from physiological-type Ca^{2+} transients. Biochim. Biophys. Acta *1366*, 5-15.

Hajnoczky G., Csordas G., Madesh M., and Pacher P. (2000). The machinery of local Ca^{2+} signalling between sarco-endoplasmic reticulum and mitochondria. J. Physiol. *529 Pt 1*, 69-81.

Heldin C.-H., Miyazono K., and Ten Dijke P. (1997). TGF-beta signalling from cell membrane to nucleus through SMAD proteins. Nature *390*, 465– 71.

Henis Y.I., Moustakas A., Lin H.Y., and Lodish H.F. (1994). The types II and III transforming growth factor-beta receptors form homo-oligomers. J. Cell. Biol. *126,* 139– 54.

Hocevar B.A., Smine A., Xu X.X., and Howe P.H. (2001). The adaptor molecule Disabled-2 links the transforming growth factor beta receptors to the Smad pathway. EMBO J. *20,* 2789– 801.

Huse M., Muir T.W., Xu L., Chen Y.G., Kuriyan J., and Massague´ J. (2001). The TGF beta receptor activation process: an inhibitor- to substrate-binding switch Mol. Cell. *8*, 671 – 82.

Itoh S., Itoh F., Goumas M.J., and Dijke P. (2000). Signaling of transforming growth factor-beta family members through Smad proteins. Eur. J. Biochem. *267,* 6954– 67.

Jouaville L. S., Pinton P., Bastianutto C., Rutter G. A., and Rizzuto R. (1999). Regulation of mitochondrial ATP synthesis by calcium: Evidence for a long-term metabolic priming. PNAS. *96,* 13809.

Jullig M. and Stott N. S. (2003). Mitochondrial localization of Smad5 in a human chondrogenic cell line Biochemical and Biophysical Research Communications *307,* 108–113.

Lai Y.T., Beason K.B., Brames G.P., Desgrosellier J.S., Cleggett M.C., and Shaw M.V., (2000). Activin receptor-like kinase 2 can mediate atrioventricular cushion transformation. Dev. Biol. *222,* 1– 11.

Liunan L., Joseph J. S., Juan C. B., Lihua H., Abanti C., Zhihong L., Chad S., Brett H. Graham and Chester W. B. (2009) Activin Signaling: Effects on Body Composition and Mitochondrial Energy Metabolism Endocrinology. *150*, 3521-3529.

Luo K., and Lodish H.F. (1996). Signaling by chimeric erythropoietin-TGF-beta receptors: homodimerization of the cytoplasmic domain of the type I TGF-beta receptor and heterodimerization with the type II receptor are both required for intracellular signal transduction. EMBO J. *15,* 4485– 96.

Luo K., and Lodish H.F. (1997). Positive and negative regulation of type II TGF-beta receptor signal transduction by autophosphorylation on multiple serine residues. EMBO J. *16,* 1970– 81.

Massague´ J. (1998). TGF-beta signal transduction. Annu. Rev. Biochem. *67*, 753– 91.

Massague´ J., and Chen Y.G. (2000). Controlling TGF-beta signaling. Genes Dev. *14*, 627– 44.

McFadzean I., and Gibson A. (2002). The developing relationship between receptor-operated and store-operated calcium channels in smooth muscle. Br. J. Pharmacol. *135*, 1-13.

McGowan T.A., and Sharma K. (2000). Regulation of inositol 1,4,5-trisphosphate receptors by transforming growth factor-beta: implications for vascular dysfunction in diabetes. Kidney Int. Suppl. *77,* 99–S103.

Meldolesi J., and Pozzan T. (1987). Pathways of Ca^{2+} influx at the plasma membrane: voltage-, receptor-, and second messenger-operated channels. Exp. Cell. Res. *171*, 271-283.

Nakao A., Afrakhte M., Moren A., Nakayama T., Christian J.L., and Heuchel R. (1997). Identification of Smad7, a TGFbeta-inducible antagonist of TGF-beta signaling. Nature *389,* 631– 5.

Oh-hora M., and Rao A. (2008). Calcium signaling in lymphocytes. Curr. Opin. Immunol. *20*, 250-258.

Pacher P, Sharma K, Csordás G, Zhu Y, Hajnóczky G. (2008) Uncoupling of ER-mitochondrial calcium communication by transforming growth factor-beta. Am J Physiol Renal Physiol. *295*(5):F1303-12.

Persson U., Izumi H., Souchelnytskyi S., Itoh S., Grimsby S., and Engstrom U. (1998). The L45 loop in type I receptors for TGF-beta family members is a critical determinant in specifying Smad isoform activation. FEBS Lett. *434*, 83–7.

Pierreux C.E., Nicolas F.J., Hill and C.S. (2000). Transforming growth factor beta-independent shuttling of Smad4 between the cytoplasm and nucleus. Mol. Cell. Biol. *20,* 9041– 54.

Rembold C.M., Kendall J.M., and Campbell A.K. (1997). Measurement of changes in sarcoplasmic reticulum [Ca^{2+}] in rat tail artery with targeted apoaequorin delivered by an adenoviral vector. Cell Calcium *21*, 69-79.

Rizzuto R., Brini M., Murgia M., and Pozzan T. (1993). Microdomains with high Ca^{2+} close to IP3-sensitive channels that are sensed by neighboring mitochondria. Science *262*, 744-747.

Rizzuto R., Pinton P., Carrington W., Fay F.S., Fogarty K.E., Lifshitz L.M., Tuft R.A., and Pozzan T. (1998). Close contacts with the endoplasmic reticulum as determinants of mitochondrial Ca^{2+} responses. Science *280*, 1763-1766.

Rizzuto R., and Pozzan T. (2006). Microdomains of intracellular Ca^{2+}: molecular determinants and functional consequences. Physiol. Rev. *86,* 369–408.

Robert V., De Giorgi F., Massimino M.L., Cantini M., and Pozzan T. (1998). Direct monitoring of the calcium concentration in the sarcoplasmic and endoplasmic reticulum of skeletal muscle myotubes. J Biol Chem *273*, 30372-30378.

Sharma K., Deelman L., Madesh M., Kurz B., Ciccone E., Siva S., Hu T., Zhu Y., Wang L., Henning R., Ma X., and Hajnoczky G. (2003). Involvement of transforming growth factor-β in regulation of calcium transients in diabetic vascular smooth muscle cells. Am. J. Physiol. Renal. Physiol. *285,* 1258–1270.

Shi Y., Wang F., Jayaraman L., Yang H., Massague´ J., and Pavletich N.P. (1998). Crystal structure of a Smad MH1 domain bound to DNA: insights on DNA binding in TGF-beta signaling. Cell *94,* 585–94.

Shimomura O. (1986). Isolation and properties of various molecular forms of aequorin. Biochem J. *234*, 271-277.

Shimomura O., Kishi Y., and Inouye S. (1993). The relative rate of aequorin regeneration from apoaequorin and coelenterazine analogues. Biochem. J. *296 (Pt 3)*, 549-551.

Streb H., Irvine R.F., Berridge M.J., and Schulz I. (1983). Release of Ca^{2+} from a non-mitochondrial intracellular store in pancreatic acinar cells by inositol-1,4,5-trisphosphate. Nature *306*, 67-69.

Szabadkai G., Bianchi K., Varnai P., De Stefani D., Wieckowski M.R., Cavagna D., Nagy A.I., Balla T., and Rizzuto R. (2006). Chaperone-mediated coupling of endoplasmic reticulum and mitochondrial Ca^{2+} channels. J. Cell. Biol. *175*, 901-911.

Szabadkai G., and Rizzuto R. (2004). Participation of endoplasmic reticulum and mitochondrial calcium handling in apoptosis: more than just neighborhood? FEBS Lett. *567*, 111-115.

Vance J.E. (2008). Phosphatidylserine and phosphatidylethanolamine in mammalian cells: two metabolically related aminophospholipids. J. Lipid Res. *49*, 1377-1387

Vance J.E. (1990). Phospholipid synthesis in a membrane fraction associated with mitochondria. J. Biol. Chem. *265*, 7248-7256.

Wang F., Kaur S., Cavin L.G., Arsura M. (2008). Nuclear-factor-kappaB (NF-kappaB) and radical oxygen species play contrary roles in transforming growth factor-beta1 (TGF-beta1)-induced apoptosis in hepatocellular carcinoma (HCC) cells. Biochem. Biophys. Res. Commun. *26,* 377 (4) 1107-12.

Wang T., Donahoe P.K., and Zervos A.S. (1994). Specific interaction of type I receptors of the TGF-beta family with the immunophilin FKBP-12. Science *265,* 674–6.

Watkins N.J., and Campbell A.K. (1993). Requirement of the C-terminal proline residue for stability of the Ca^{2+}-activated photoprotein aequorin. Biochem. J. *293 (Pt 1)*, 181-185.

Wicks S.J., Lui S., Abdel-Wahab N., Mason R.M., and Chantry A. (2000). Inactivation of smad-transforming growth factor beta signaling by Ca^{2+}-calmodulin-dependent protein kinase II. Mol. Cell. Biol., *20,* 8103– 11.

Wieckowski M.R, Giorgi C, Lebiedzinska M, Duszynski J, Pinton P.(2009). Isolation of mitochondria-associated membranes and mitochondria from animal tissues and cells. Nat Protoc. *4*(11):1582-90

.